Final report

1.1 Project details

Project title	**New Coatings for Biomass Firing**
Project identification	14-I 64014-0109
Name of the programme which has funded the project	EUDP 14-I. Programme area: Biomass
Project managing company/institution	DTU Mekanik, Niels Koppels Allé 404, 2800 Kgs. Lyngby
Project partners	Added Values P/S Refa Energi A/S Verdo A/S Burmeister & Wain Energi A/S – replaced by BWSC A/S
CVR (central business register)	30060946
Date for submission	November 13, 2018

1.2 Short description of project objective and results

The project aimed to develop and demonstrate new corrosion resistant coating materials for heat exchangers (superheaters) in biomass fired CHP plants. Very promising systematic laboratory results had indicated that coatings based on Al and/or Ni could to enable improved economy in biomass firing through increased reliability, prolonged lifetimes and higher efficiency.

Processes were developed to produce coatings on full scale superheater tube sections (length 200 mm), which were installed in two different biomass fired CHP plants for up to two years. Unfortunately, all the coatings failed due to either spallation or corrosion, which demonstrate that the laboratory tests could not mimick the much harsher materials loads in real plant in a realistic way.

Projektet sigtede mod at udvikle og demonstrere nye korrosions resistente coating materialer til overhedere i biomassefyrede kraftvarmeværker. Meget lovende systematiske laboratorie resultater havde indikeret, at coatinger baseret på Al og/eller Ni kunne bidrage til at forbedre økonomien ved biomasse fyring, igennem forbedret driftssikkerhed, forlængede levetider og forbedret effektivitet.

Processer blev udviklet til at fremstille fuld skala coatede overhederrør (længde 200 mm), som blev indsat i to forskellige bomasse fyrede kraftvarmeværker i op til to år. Desværre fejlede alle coatings ved enten afskalning eller korrosion. Dette demonstrerer, at laboratorieafprøvningen ikke kunne genskabe de meget skrappere materialebelastninger i et kraftværk på realistisk vis.

1.3 Executive summary

Biomass contains highly aggressive species, which cause severe corrosion of heat exchangers (superheaters) in boilers at steam temperatures higher than 540^{0}C. Thus, high temperature corrosion is a major challenge for biomass-based heat and power production leading to reduced reliability, increased maintenance costs and limited efficiency.

State of the art materials solutions for superheaters in biomass fired boilers are 18%Cr austenitic steels. Based on new understanding of corrosion mechanisms in biomass firing the present project aimed to develop and demonstrate new innovative coatings containing aluminium and/or nickel. Systematic small-scale laboratory tests had indicated that such coatings could significantly reduce corrosion rates in biomass fired power plants, which could enable:

- prolonged heat exchanger lifetimes and improved reliability of existing conventional CHP plants
- avoiding reduction of steam temperatures in large central advanced power plants as a consequence of their conversion from coal to biomass
- construction of new biomass boilers with higher operating temperatures and improved efficiency

Coating processes were developed at DTU Mechanical Engineering and tube sections (200 mm length) were coated with Ni by electroplating and subsequently Al was diffused into the surface of the Ni plating by pack aluminizing.

Tubes sections coated with Ni and with NiAl were installed in the superheaters of two different biomass fired CHP plants at Refa Energi in Maribo Sakskøbing (MSK) and at Verdo in Randers. The plants were selected since they had very different operating conditions: Whereas MSK had daily start-stop cycles and operated at steam temperature up to 540ºC, Randers operated continuously at steam temperatures up to 520ºC with only few stops in the heating season. Also the plants fired different biomasses (Straw/grass seed chaff at MSK and Wood chips or pellets at Randers).

Added Values selected the specific installation sites in the plants based on superheater model calculations, which identified positions, where the most severe corrosion could be expected. BWE welded the tubes into the superheaters after approval of the experiment with the pressure vessel authorities (Arbejdstilsynet). Tubes were tested up to two years with partial replacement after one year.

Investigations of the extracted tubes showed that both the Ni and the NiAl coatings spalled at MSK during the first year of operation, most probably due to the highly intermittent operation, which leads to cyclic thermal stresses in the coatings and a predominantly mechanical failure. At Randers, the NiAl coatings survived the first year of operation, due to lower temperature and less intermittent operation. However, during the second year of operation the NiAl coatings at Randers failed completely due to corrosion attack, which shows that the protective corrosion behavior seen in the laboratory could not be confirmed in plant.

The Ni coatings performed better in Randers, but they were found to offer only rather marginally reduced corrosion rates as compared to uncoated tubes.

As such the in-plant testing proved to be much harsher than the simplified laboratory testing. Thus, future materials development for improved corrosion resistance in biomass firing must consider tests in corrosive environments much closer to the conditions in real plant.

A feasibility study by Added Values has quantified the considerable potential economic gains over plant lifetime, which can be foreseen with either improved efficiency (10-300 MDKK) or reduced O&M costs (5-30 MDKK) of biomass fired CHP plants based on improved materials.

1.4 Project objectives

1.4.1 Background

The overall goal for the Danish energy system is to become fully independent of fossil fuels by 2050 and that all fossil fuels for electricity and heat production should be phased out by 2035. An essential tool in this respect is to convert central power plants from coal to biomass firing (mainly wood pellets), and to use various forms of biomass in smaller decentralized combined heat and power (CHP) plants.

Biomass contains highly aggressive species, which cause severe corrosion of the heat exchangers (superheaters) exposed to hot flue gases in boilers. Thus, high temperature corrosion is a major challenge for biomass based heat and power production.

The efficiency of thermal power plants improves with increasing temperature and pressure of the process steam. In state of the art biomass fired CHP plants combustion of the biomass (straw or wood chips) takes place in grate fired boilers. Since 1993 biomass firing in Denmark has increased considerably, and biomass fired boilers with gradually more advanced steam temperatures and better efficiency have been constructed by Danish boiler makers.

Systematic microstructure investigations of materials samples from in-plant tests have identified austenitic steels alloyed with 18%Cr and 10%Ni as the state of the art materials solution for superheaters in biomass fired boilers. The 18%Cr steels allow steam temperatures of 540^0C, but even at this rather limited temperature strong corrosion can appear leading to reduced reliability and increased maintenance costs.

Prior to the present project, systematic research at DTU including materials development based on fundamental understanding of corrosion mechanisms, had identified materials, which could potentially survive longer and allow increased steam temperatures in the harsh corrosion environments.

Superheater materials coated with the identified materials were tested in laboratory in simulated biomass firing conditions and showed very low corrosion rates compared with 18%Cr steels. As such the identified coating materials represented materials solutions, which could potentially enable significantly improved reliability and efficiency of biomass fired power plants.

Since the coating materials had only been manufactured in small scale and tested under simplified laboratory conditions, a number of effects from real boiler applications were not included:

- Thermal cycling as a result of fluctuations in temperature and start/stop procedures
- Temperature gradients across the superheater tube wall and deposits
- Influence of deposit formation and cleaning procedures such as soot-blowing
- Influence of complex (fluctuating) flue-gas chemistry and other deposits than in laboratory, e.g. sulphur containing deposits
- Long-time depletion of vital elements through interdiffusion between coating and substrate

Thus, the present project focused on upscaling and long-term testing of the identified coating materials in two real biomass fired boilers at Refa Energi in Maribo-Sakskøbing and at Verdo in Randers.

1.4.2 Objectives

The project objectives were:

- to further develop coating materials with improved corrosion resistance in biomass firing as compared with state-of-the art 18%Cr steels.
- to develop coating technologies for the deposition of these materials on superheater tubes
- to demonstrate the viability of coated superheater tubes in exposure tests in real biomass fired boilers for up to two years.

1.4.3 Implementation

The project was defined by DTU Mechanical Engineering. Four project partners were identified, who had the experience and infrastructure to support the in-plant testing, i.e: consultant AddedValues P/S, who has experience in superheater lifetime estimations; boilermaker Burmeister & Wain Energy A/S, who is a major supplier of biomass fired boilers; and finally Refa Energi A/S and Verdo Randers, who are operators of biomass fired boilers.

The project was organised into five work packages with specific objectives and responsible partners:

WP1: Materials development (DTU Mechanical Engineering)
The identified coating materials will be further developed on the laboratory scale with special emphasis on mechanical stability of the coatings and interdiffusion between coating and substrate. Modified coatings may be designed to optimize these properties without impairing the corrosion resistance. Fundamental models for the long-term stability of coatings will be developed and validated based on the investigations of service-exposed materials.

WP2: Process development (DTU Mechanical Engineering)
Process parameters for the coating process will be developed in order to upscale the coated components from small test coupons to superheater test tubes of some 250 mm length. The coating process (mainly pack cementation) will be optimized based on process models and laboratory experiments. Two sets of test tubes for installation in the power plants will be manufactured.

WP3:Superheater demonstration (Added Values, BWE, Refa Energi, VERDO)
Test tubes with coatings will be installed in selected superheaters of Maribo Sakskøbing CHP and Randers CHP. Together with the boiler owners Added Values will select the optimum installation sites in the boilers. Added values will evaluate boiler operating data, deposit formation, etc. after the tests. BWE will install and remove the test tubes.

WP4: Evaluation and feasibility (Added values, BWE, DTU Mechanical Engineering)
The overall performance of the coating materials will be evaluated with the aim to identify necessary technical steps for implementation of the materials in full scale application (e.g. joining and repair technologies). Furthermore, an evaluation of the economic feasibility (manufacturing costs vs. savings from prolonged lifetime or improved efficiency), and a plan for commercialization of the coating technology will be made.

WP5: Project Management, reporting and dissemination (DTU Mechanical Engineering)
Coordination of work packages, facilitation of dissemination activities and reporting to EUDP.

The project was initiated on September 1, 2014 and finished on June 30, 2018 with six months delay according to the original project plan.

The research part of the project was carried out by staff at DTU Mechanical Engineering. A ph.d. student, Duoli Wu, was hired for the project and he carried out his ph.d. project as part of the EUDP project. The ph.d. project was initiated on December 15, 2014, and the thesis

was handed in on February 28, 2018 and successfully defended on April 6, 2018. The ph.d. student was on paternal leave from September 15, 2016 to December 15, 2016. This caused the overall EUDP project to be delayed according to the original plan. Otherwise, all deadlines and milestones in the project related to the test installation and sample removal were met.

Risks in the project were mainly related to the uncertainties of the performance of the selected coatings in actual plant, which were tested as the main purpose of the project. The coatings did not fulfil the expectations, since, as described in detail below, the plant conditions were much harsher than the laboratory conditions.

In the course of the project the boilermaker BWE went bankrupt early 2017. However, the company was taken over by BWSC A/S, who also took over the responsibilities of BWE in the project to remove the last set of test samples from the plants and provide input to the feasibility study. Otherwise, only minor unforeseen problems occurred in the project.

1.5 Project results and dissemination of results

1.5.1. Background

From 1997 systematic microstructure investigations of materials samples from in-plant tests in biomass fired boilers have been carried out at the Technical University of Denmark (DTU) in close collaboration with the major Danish utility companies. It was concluded that amongst the existing superheater tube materials, austenitic steels alloyed with 18%Cr and 10%Ni offer the best corrosion resistance. Even for these steels the corrosion rate increases drastically when the temperature is increased [1], figure 1.

The investigations of in-plant tested materials further showed that the usual approach to increase the Cr-content in order to reduce corrosion rates is not applicable to biomass induced corrosion; on the contrary selective internal Cr-corrosion and increased overall corrosion rates were observed with increased Cr-content above 18% [2], figure 2.

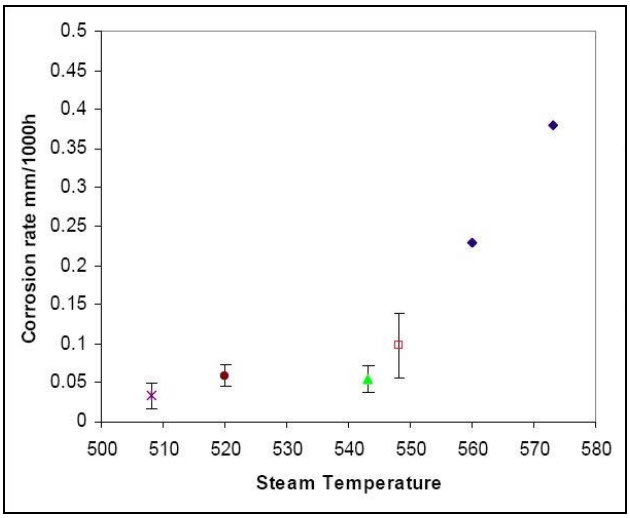

Figure 1. *Corrosion rate of steel TP347HFG superheater tubes inserted in Danish biomass fired power plants as a function of steam temperature. [1]*

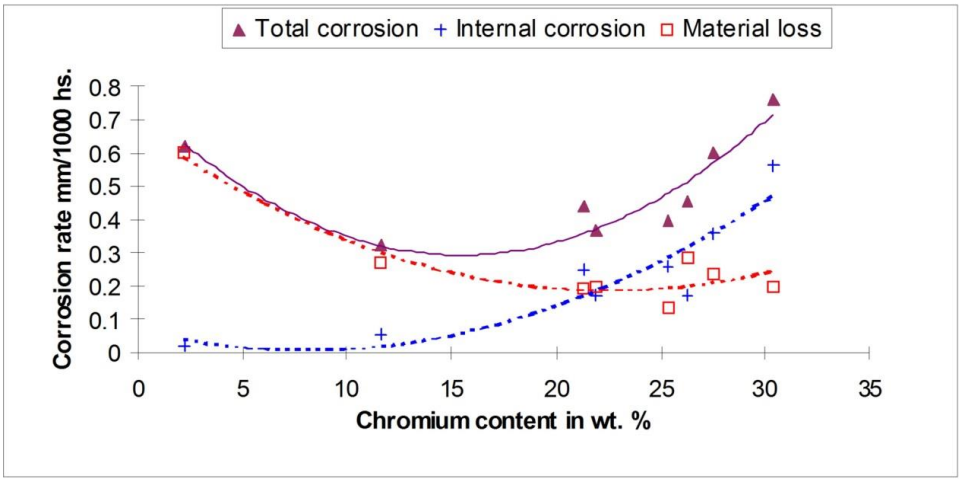

Figure 2*: Corrosion rates of alloys with different Cr-content. The minimum overall corrosion rates lie at the Cr-level of the 18-10 type steels presently in use. For lower Cr contents a high material loss is observed and at higher Cr-contents internal corrosion attack increases. Based on data from [2].*

1.5.2 Corrosion mechanism

Several mechanisms have been proposed to describe biomass induced corrosion. According to the so-called active oxidation or chlorination cycle [3], chlorine is transported through the oxide layer, underneath which it can then form volatile metal chlorides that diffuse out through the oxide layer where they are oxidized. Thus, chlorine is released and free to again enter the material and re-start the chlorination cycle. This focus on the chlorine that is contained in biomass such as straw and wood pellets has led to the use of the name chlorine induced corrosion. However, newer studies indicate that not only chlorine is active in the

corrosion but that potassium plays a major role in the initial breakdown of the protective oxide layer on superheater steels. Controlled laboratory exposures have shown that Cr-rich oxide reacts with KCl to form K_2CrO_4 resulting in breakaway oxidation and formation of non-protective oxides [4-9]. The studies show that breakaway oxidation begins already within the first hour of exposure at 600°C [5].

Studies at DTU of samples from steel TP347HFG tubes (18%Cr, 10%Ni) used in superheater test sections at Amagerværket unit 1 underline the influence of K on the corrosion also in real plant conditions; K can be found alongside Cl in grain boundaries at the corrosion front, see figure 3. The tubes were exposed for 5900 hours at a steam temperature of 535°C. Even under these relatively mild conditions the steel was not able to maintain a protective oxide layer and significant internal corrosion occurred.

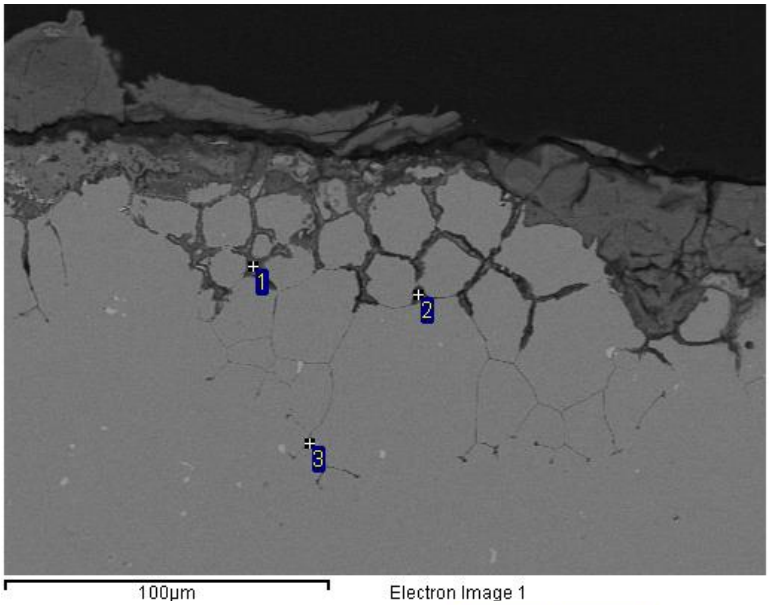

Spectrum	O	Si	S	Cl	K	Cr	Mn	Fe	Ni	Nb
1	17.2	1.7		2.3	4.0	30.7		20.3	9.2	14.7
2	17.6	1.3	1.1	3.6	2.7	45.5		23.0	5.2	
3	0.6					23.9	1.5	64.6	9.4	

Figure 3. *Biomass induced corrosion on a TP347HFG steel tube from a superheater. Extensive attack along grain boundaries, K and Cl are located in the boundaries at the corrosion front; results of composition measurements at points 1-3 are shown in table 1. SEM backscatter contrast image. The table shows compositions in mass percent measured with SEM-EDX at the positions indicated.*

1.5.3. Materials and coating systems

At DTU fundamental studies of the corrosion mechanism and screening of new candidate materials systems were carried out in the DSF funded center "GREEN - Center for power generation from renewable energy" [9-12] and in the KME511 project [13]. The research indicated that alumina and silica forming alloys or coatings could be promising alternatives to the present state of the art chromia forming steels. Similar promising trends have been found by Li and Spiegel et al. [14-15]. With the realization of the role of K in the breakdown of the oxide scale an obvious analogy to NaCl induced hot corrosion can also be drawn. For this type of corrosion it is known that increased Cr-content increases the corrosion rates because of direct reaction between NaCl and Cr_2O_3 to form Na_2CrO_4 [16-17]. Furthermore Hiramatsu et al. [17] found beneficial effects from addition of Al, Si and Ni to stainless steel grades. Sato et al. [18] found good resistance of siliconized stainless steels exposed to NaCl-KCl mixtures at 600°C.

In the KME511 project Ni_2Al_3 intermetallic coatings made by pack cementation aluminizing were tested against KCl induced corrosion at 600°C under well controlled laboratory conditions in a simplified environment mimicking that of biomass firing (Gas: 5% O_2, 40% H_2O, deposit: 0.10 mg/cm^2 KCl). In contrast to results for steels no breakaway oxidation was observed for exposure times up to 168 hours [19], cf. figure 4. In comparison, breakaway has been observed after 1h at the same conditions for the 18Cr-8Ni steel 304L [5]. The results

indicate that the Ni_2Al_3 nickel-aluminide can be resistant towards KCl induced corrosion at 600°C. KCl evaporates during the experiment resulting in the small weight loss observed for the Ni_2Al_3 coated samples. Steel 304L and pure Ni, which were included for reference both experience breakaway oxidation resulting in substantial mass gains.

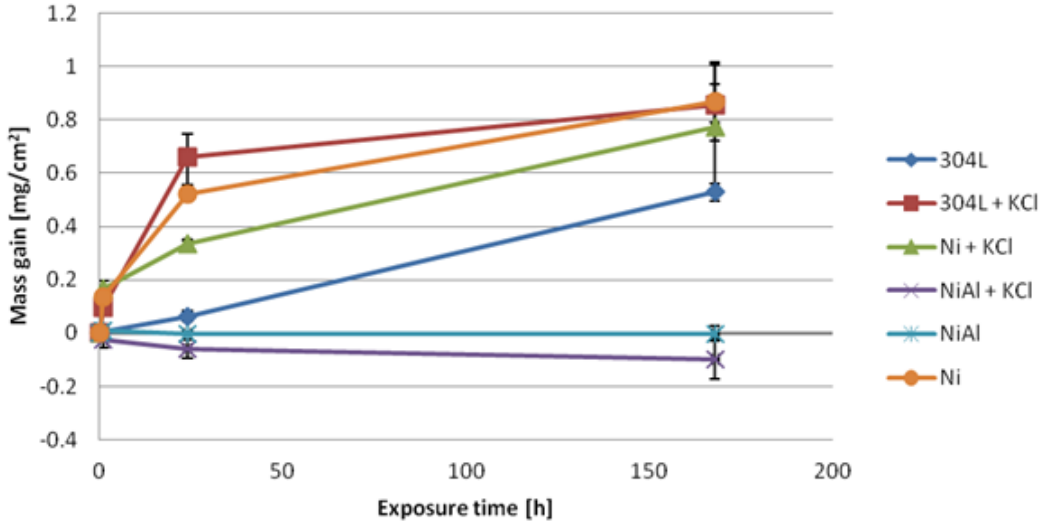

Figure 4: *Measured mass gains for materials exposed at 600°C with or without KCl deposit under controlled laboratory conditions done at HTC Chalmers during the KME511 project (Gas: 5% O_2, 40% H_2O, deposit: 0.10 mg/cm^2 KCl) [19].*

Transmission electron microscopy (TEM) carried out on thin foils produced by focused ion beam milling (FIB) reveals a thin (less than 400 nm at the thickest place) oxygen-rich layer on the surface of the exposed Ni_2Al_3 coated sample after 168 hours exposure with KCl deposit, see figure 4. EDX measurements and electron diffraction reveal that a mixed $K_xAl_yO_z$ oxide has formed in some parts of the layer, but the layer remains thin indicating very limited reactivity and a protective behavior. [19]

In addition, in situ plant exposures of various materials have revealed that corrosion leads to preferential attack of chromium and iron, while Ni is left behind as a porous substrate, which indicates that Ni has less reactivity in KCl environments and could contribute to a protective coating [20].

Based on these very promising results, the first group of coating systems selected for in-plant testing in the present project was based on NiAl and pure Ni.

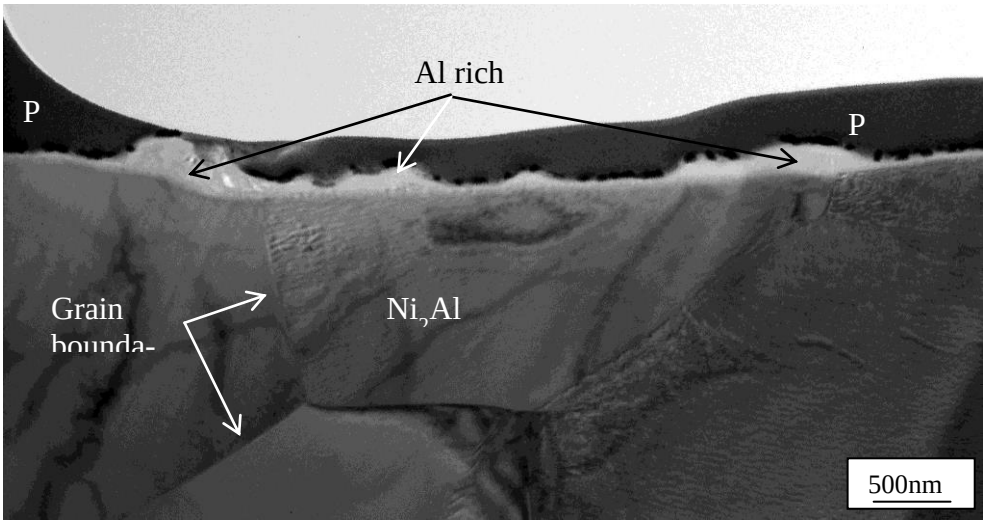

Figure 5: *TEM image of the surface of an Ni_2Al_3 coated sample after 168 hours exposure to gas and KCl deposit mimicking the environment during biomass combustion (Gas: 5% O_2, 40% H_2O, deposit: 0.10 mg/cm^2 KCl) [19].*

1.5.4. Coating technology

The coatings tested in the KME511 project were manufactured by pack cementation. Pack cementation is an efficient and inexpensive method for surface modification. The sample to be coated is embedded in a powder mix (pack) and then heated to process temperature, typically in a retort. In the pack volatile compounds of the element to be inserted are formed by reaction with an activator, thereafter the volatile compounds decompose at the sample surface leaving the element to diffuse into the surface. Pack cementation is a well-established coating method that was used for aluminizing as early as 1911 [21]. Today, both siliconizing and aluminizing by pack cementation are industrially available and aluminizing of tubes up to 18.5 meter long can be carried out [22]. The pack aluminizing can be run at temperatures below 700°C thus enabling treatment of both ferritic and austenitic steels without introducing detrimental microstructure effects. Siliconizing is typically done at higher temperatures, e.g. above 900°C.

Direct aluminizing of steel will result in the formation of Fe-Al intermetallic phases; i.e. FeAl or Fe_2Al_5 [24, 25]. On ferritic steels the iron-aluminides, however, suffer from aluminium-loss through interdiffusion into the bulk alloy [22, 25]. This effect can be mitigated by the use of a Ni barrier layer deposited by electroplating, this then leads to the formation of nickel aluminides like Ni_2Al_3 [21-234].

1.5.5. Coating of sample tubes

Electroplating and pack cementation were selected as the coating procedures to be applied for the majority of the tubes to be installed in the power plants as part of the present project. A new tube furnace was acquired, which could allow pack cementation of tube sections of 200 mm length, figure 6.

Figure 6. *Furnace for pack cementation*

Two different austenitic stainless steels, Esshete 1250 and TP347H, were used for the superheater tubes in the biomass fired power plants. Their nominal chemical compositions are given in Table 1 as specified by SANDVIK data sheets [26]. Sections with a length of 200 mm were cut from these two steel tubes (Esshete 1250: outer diameter (OD) 32 mm, inner diameter (ID) 19 mm; TP347H: OD 33 mm, ID 22 mm).

Table 1. *Nominal chemical composition of Esshete 1250 and TP347H (wt. %, Bal. Fe).*

	Cr	Ni	Mn	Nb	Si	C	Mo	V	S	P	B
Esshete	15	9.5	6.3	1.0	0.5	0.1	1.0	0.3	≤0.015	≤0.035	0.005
TP347H	17.5	10	1.7	0.7	0.6	0.05			≤0.015	≤0.030	

The Ni_2Al_3 coatings were applied to the cut sections of superheater tubes by a two-step process where nickel was first electroplated followed by low temperature pack aluminizing. The samples were grit blasted before the cleaning process was started. The samples were cleaned in anodic degreaser for 3 minutes followed by chemical activation in dry acid for 3 minutes. A pre-plating process was performed in a Woods nickel strike bath (5 minutes with a current density of

6 A/dm^2) and then a Watts nickel-plating bath was used for the final nickel-plating process. The final plating was performed at 45 ^{O}C with a current density of 6 A/dm^2 for 100 minutes. The samples were rinsed in ethanol after processing. The Ni plated tubes were then heat-treated at 650 ^{O}C for a period of 1 h in a gas mixture of Ar and 10 vol. % H_2 to strengthen the diffusion bonding between the steel and the nickel layer prior to pack aluminizing.

For aluminizing several experiments with optimization of the coating process were performed at DTU [27], which led to the following process parameters: The Ni coated tube sections were embedded in a pre-mixed pack powder (10 wt. % Al + 8 wt. % $AlCl_3$ + 82 wt. % Al_2O_3), which was put into a cylindrical metal crucible. The crucible was then placed in the tube furnace with flowing argon. The furnace was heated to 650^{O}C with a heating rate of 18^{O}C/min, and maintained at this temperature for 6 h. The samples were afterwards cooled inside the furnace by switching off the power while maintaining the argon flow. After aluminizing, the Ni_2Al_3 coated tubes were ultrasonically degreased in acetone and subsequently driedwith ethanol. The coating was removed by machining from a 2 cm wide area from both ends of the Ni_2Al_3 coated tubes prior to welding. The tubes after preparation are shown in Figure 7. The discoloration area on the Ni_2Al_3 tubes (Figure 7a) is due to a thin (around 2 µm) Al_2O_3 layer, which was probably related to surface oxidation during furnace cooling or the last part of the pack aluminizing process. Destructive examination from similar locations revealed that the Ni_2Al_3 coating beneath the thin layer was intact and uniform. The bubbles visible on Ni and Ni_2Al_3 tubes (Figure 7b) were probably due to hydrogen gas introduced during the Ni-plating process.

Figure 7. *Appearance of the first set of test tubes for (a) Esshete 1250 and (b) TP347H.*

The test tubes were installed and removed in two CHP plants during yearly overhauls in the summer. The first group of tubes was installed in the summer of 2015. One set of tubes was removed by cutting from the middle of the uncoated tube during the summer overhaul in 2016 and the other set of the tubes were removed during the summer overhaul in 2017. The second group of tubes was installed in the summer of 2016 and was removed during the summer overhaul in 2017. An overview of the tested tubes is given in Table 2.

Table 2. *Overview of the tubes exposed in two power plants*

Plant	Material	2015-2016	2016-2017	2015-2017
Randers	Esshete 1250	Uncoated tube Ni coated tube Ni_2Al_3 coated tube	Ni_2Al_3 coated tube Preoxidized Ni_2Al_3 coated tube CeO_2-dispersed Ni_2Al_3 coated tube Nitrided tube	Uncoated tube Ni coated tube Ni_2Al_3 coated tube
MSK	TP347H	Uncoated tube Ni coated tube Ni_2Al_3 coated tube	Ni_2Al_3 coated tube Preoxidized Ni_2Al_3 coated tube CeO_2-dispersed Ni_2Al_3 coated tube Nitrided tube	Uncoated tube Ni coated tube Ni_2Al_3 coated tube

Since the results from the first tube set was only available after year one, the second group of coatings had to be selected based on further laboratory tests. More advanced laboratory tests and interdiffusion tests indicated that diffusion between the AlNi layers and the Ni layer could lead to the formation of Kirkendall porosities [28]. Thus, CeO_2 particles, were dispersed in the Ni layer during electroplating to act as diffusion barriers.

Furthermore, the preoxidising the NiAl coated tubes to provoke the formation more stable aluminium rich oxides and nitriding to test the effect of nitrogen rich layers on corrosion was included in the second group of coatings.

1.5.6 In-plant testing

Tubes were tested in two different biomass fired combined heat and power (CHP) plants, Randers CHP and Maribo-Sakskøbing CHP (MSK). The nominal and actual operating conditions of the two plants are shown in Table 3.

The two plants were chosen for testing because they represent highly different operating conditions both by fuel and operating mode, Table 3. The fuel fired in Randers was composed of 90 wt. % wood chips and 10 wt. % wood pellets, while 79 wt. % wheat straw and 21 wt. % grass seed chaff was fired in MSK. Wood chips and wheat straw are the most abundant biomass resources in Denmark. A general overview of the major chemical elements present in the biomass utilized in Randers and MSK is shown in Table 4. The chemical compositions from Randers were actual measurements of the fuel used at the plant in 2012 [29] whereas those for MSK were taken from the ECN database for wheat straw and grass seed chaff [30]. The chemical compositions were measured on dry basis and the overall values were calculated based on the percentage of different biomass resources used.

Table 3. *The nominal and actual operating conditions of the two plants.*

Nominal conditions	Randers	MSK
Fuel	Wood chips/pellets	Straw/ grass seed chaff
Steam pressure [bar]	110	95
Outlet steam temperature [°C]	520	540
Steam mass flow [kg/s]	29	12.5
Superheater material	Esshete 1250	TP347H
Tube dimensions [mm] OD x wall thickness	31.8 x 6.3	33.7 x 5.6
Superheater design	Vertical hanging	Vertical hanging
Actual operating conditions		
Exposure time [h]	7100 (T_{steam}>450°C)	6200 (T_{steam}>500°C)
Average steam outlet temperature. [°C]	502	536
Average outlet steam temperature where the test tube is installed. [°C]	512	544
Test tube average metal temperature [°C] (bottom-top)	515-518	543-546
Start/stop cycles	1	213

Table 4. *Fuel data for Randers and MSK.*

Power Plants	Randers			MSK		
Biomass resources	Wood chips	Pellets	Overall value	Wheat straw	Grass seed chaff	Overall value
Moisture, wt.%	6.50	6.25	6.48	8.70	11.24	9.23
Ash, wt.%	0.80	3.82	1.10	2.80	13.38	5.02
Chlorine, Cl, wt.%	0.02	0.06	0.02	0.23	0.14	0.21
Sulphur, S, wt.%	0.01	0.09	0.02	0.15	0.18	0.16
Carbon, C, wt.%	49.60	47.68	49.41	47.79	41.33	46.43
Hydrogen, H, wt.%	6.00	6.05	6.00	5.91	5.49	5.82
Nitrogen, N, wt.%	0.17	1.11	0.26	0.68	1.69	0.89
Oxygen, O, wt.%	43.00	41.17	42.82	42.07	37.79	41.17
Potassium, K, wt.%	0.10	0.66	0.15	0.98	0.71	0.92

The operating conditions for the two CHP plants are also very different. At Randers it is preferred to run at part load rather than shutting the plant down when the heat demand is low, and as shown in Figure 7, the plant had only one shutdown during each exposure period.

However, at MSK the plant is run under cyclic conditions with daily start/stops in the beginning and end of the heating season (Figure 9). This means that at MSK the boiler runs at full load when in operation. This difference in operating conditions can also be seen when comparing the temperature histograms, which is broad for the Randers plant, and narrow for the MSK plant (Figure 10).

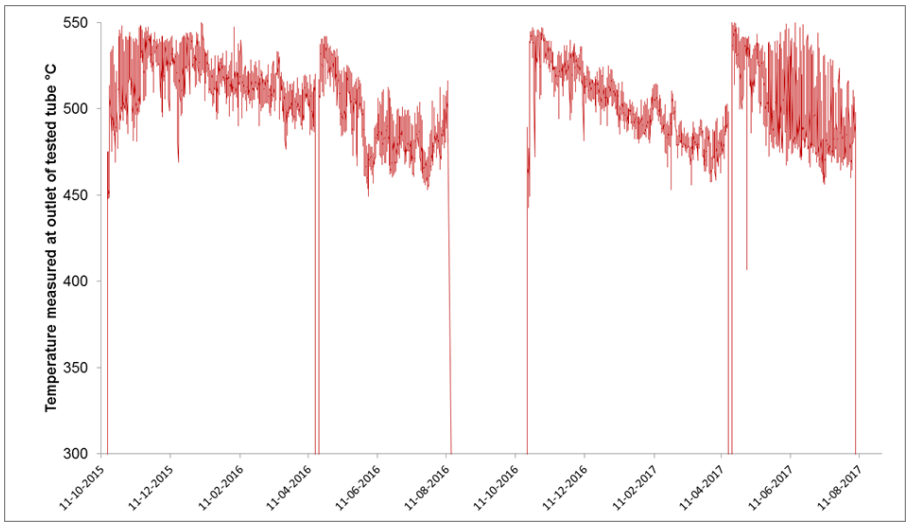

Figure 8. *The outlet steam temperature data for the exposure period in Randers.*

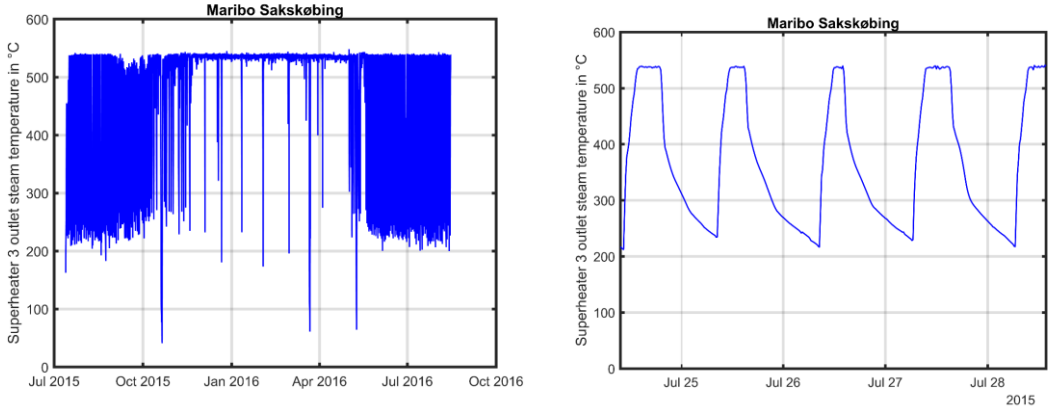

Figure 9. *The outlet steam temperature data for MSK, showing the whole exposure period (left) and the daily cycle (right).*

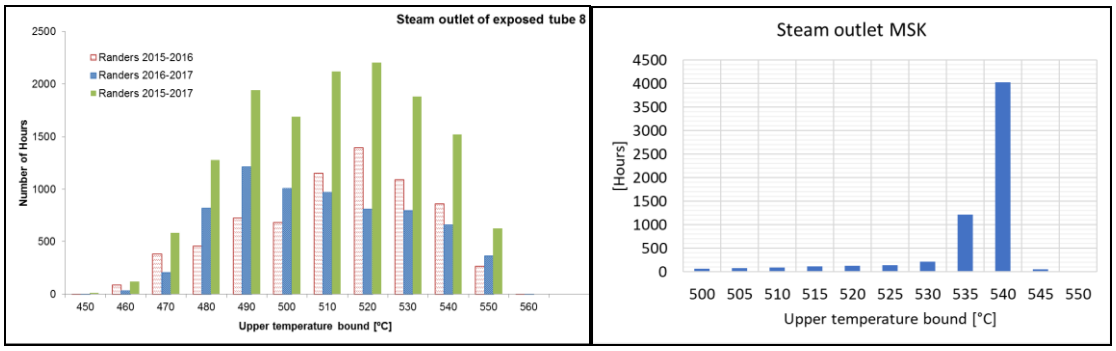

Figure 10. *Temperarure histograms for the whole exposure period for Randers (left) and for the first year for MSK (right)*

1.5.6.1 Randers test tube

A cross-section of the Randers boiler, as well as superheater 3 (SH3) with the test tube is shown in Figure 11. SH3 has 14 parallel tube banks and the test tube was placed in bank no. 8, close to the center of the boiler. The position of the test tube was chosen based on temperature analysis of the superheater with considerations to geometrical limitations. The temperature analysis was performed using a numerical tube model where the tube internal and external metal temperatures are calculated from inlet to outlet, under given boundary condi-

tions (inlet/outlet steam temperature, steam side oxide thickness, material properties, heat flux profile, pressure, etc.) [31]. The oxide thickness is calculated in the model as a simulation from new to actual time of operation. The oxide growth kinetics is based on tube investigations from other plants with the same type of materials. A bimodal flux profile was assumed for the Randers analysis, due to the double pass of the SH tubes. The heat flux is assumed to be the highest near the bottom (closest to the grate) and the lowest at the boiler roof. The resulting temperature profile from inlet to outlet at a steam outlet temperature of 512°C is shown in Figure 12. The metal temperature, which controls the corrosion process, is the highest in the high flux areas, and peaks around 19 m from the inlet (with the chosen flux profile). The test tube was placed 18-20 m from the inlet as indicated in Figure 6, i.e. at the peak metal temperature. The position is easy to access and the tube outlet temperature is measured with a thermocouple.

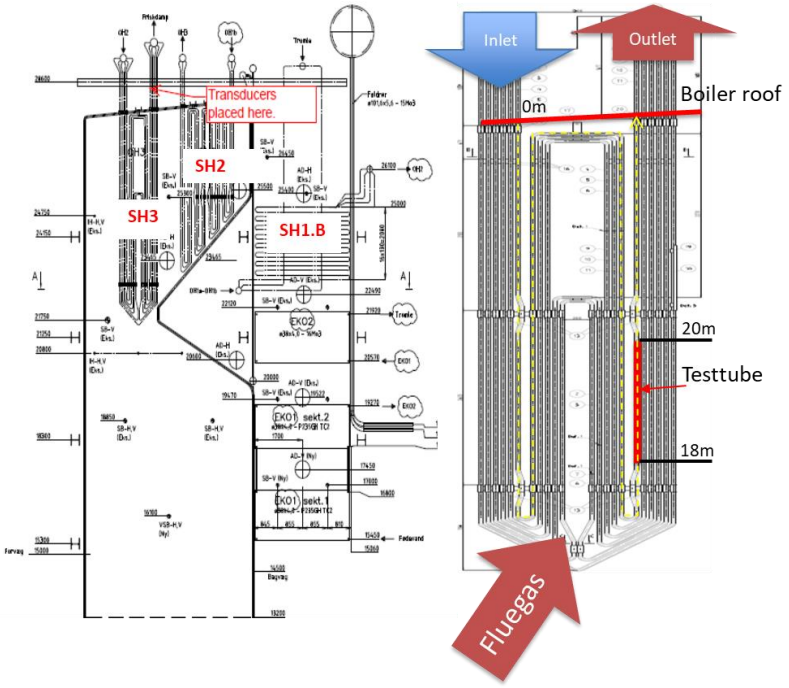

Figure 11. *Cross-section of Randers boiler and position of the test tube on superheater 3.*

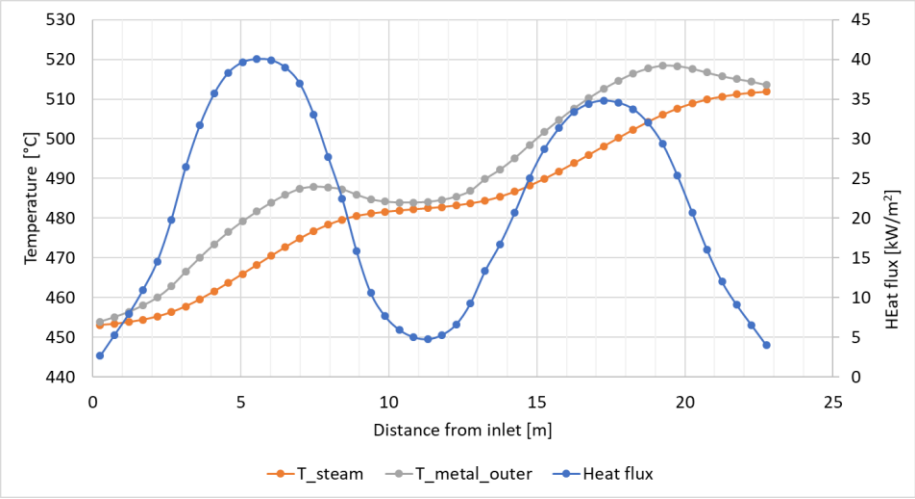

Figure 12. Calculated steam and outer metal temperature of SH tube from inlet to outlet in Randers. The test tube was placed from 18-20 m from the inlet.

1.5.6.2. MSK Test tube

In Figure 13, a cross section of the MSK boiler and superheater 3 (SH3) is shown. At MSK, SH3 is placed in the second pass of the boiler as indicated. SH3 has 8 parallel tube banks and the test tube is placed in bank no. 4, close to the center of the boiler. The position of the test tube was chosen in the same way as in Randers. For MSK a parabolic heat flux was chosen. This profile was chosen based on the assumption that the heat flux (flue gas flow and

temperature) is slightly higher near the nose of the boiler compared to the boiler roof. The results of the temperature analysis are shown in Figure 14. Due to the lower overall heat input, and lower steam mass flow, the average heat flux is lower at MSK than in Randers. With the chosen flux profile, the outer metal temperature is almost parallel to the steam temperature and reaches the highest value at the superheater outlet. The test tube was placed close to the outlet, approximately 0.4 m under the boiler roof. This area is also reported from the plant operator to have high corrosion rates. Analysis of temperature measurements from tubes adjacent the test tube indicates that the steam temperature is approximately 8°C above the average steam temperature. Therefore, 8°C has been added to the average steam temperature in this analysis (see Table 2).

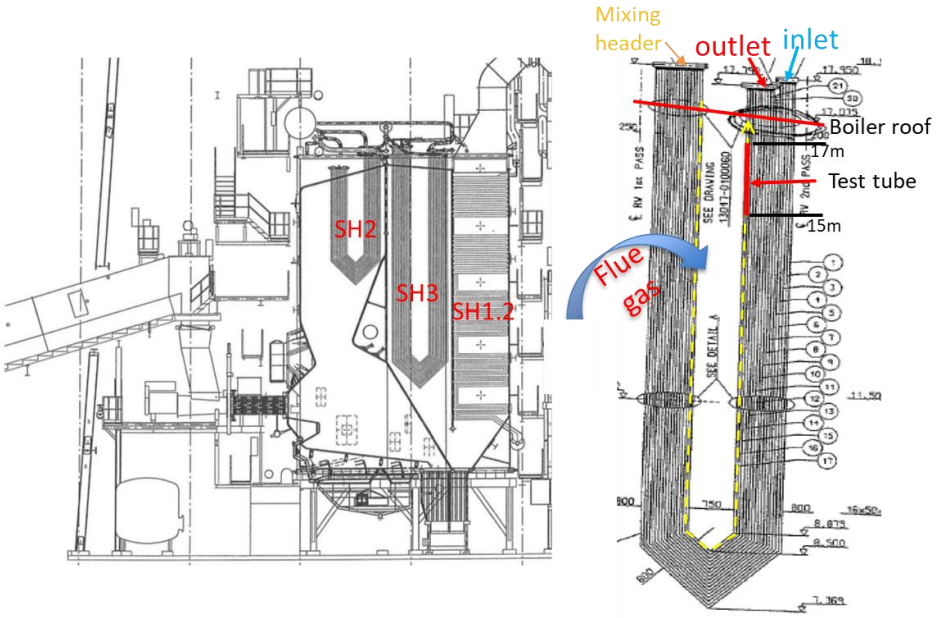

Figure 13. *Cross-section of MSK boiler and position of the test tube on superheater 3.*

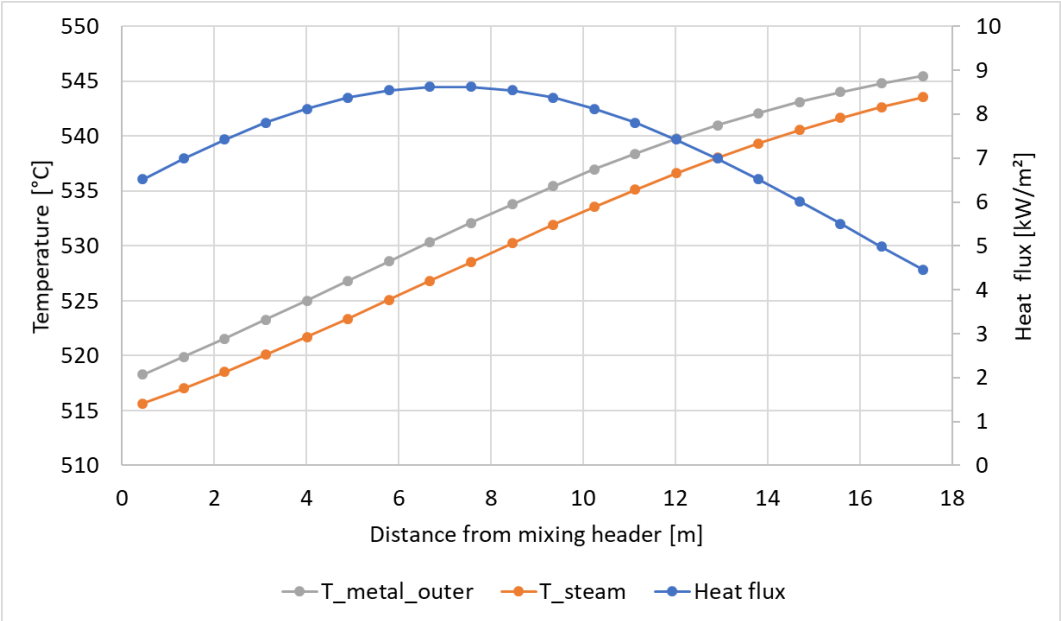

Figure 14. *Calculated steam and outer metal temperature of SH tube from mixing header to outlet in MSK. The test tube was placed from 15-17 m close to the outlet.*

1.5.7 Results from in-plant testing

After the test installation had been approved by the pressure vessel authorities (Arbejdstilsynet) the tubes were welded into the superheaters at the selected positions. Figure 15 shows the installed tubes.


a)

b)

Figure 15. *Test tubes welded into the superheaters at a) MSK and b) Randers.*

1.5.7.1 Sample preparation and characterization

After plant exposure, the test tubes were removed from the Randers and MSK boilers. The tube sections were cut into thin rings (1 cm) in dry condition and were embedded in epoxy resin. In order to reduce dissolution of water-soluble compounds, grinding and polishing were performed using absolute ethanol as lubricant. Grinding was performed using SiC paper, while polishing was done with diamond slurry until a final step of 1 µm diamond. The cross-sections were examined using a scanning electron microscope (FEI Inspect S) equipped with energy dispersive X-ray Spectroscopy (Oxford Instruments 50mm^2 X-Max silicon drift detector) for chemical analysis (SEM-EDX). Image acquisition was performed in back-scattered electron (BSE) mode with high vacuum. Deposits from both tubes were photographed using an Olympus BH-2 stereomicroscope. The deposits were prepared in cross-sections by dry polishing up to 4000 grit paper, and investigated with scanning electron microscopy. In addition the surface of deposits adjacent the tube were examined with SEM-EDX.

1.5.7.2 Unexposed tubes

Cross sectional views of the Ni and Ni_2Al_3 coated samples are shown in Figure 16. The Ni coating consisted of a single Ni layer with a thickness of 135(±5) µm. The Ni_2Al_3 coating, with a double layer structure, was adherent to the steel. The double layer coating consisted of an outer Ni_2Al_3 layer (thickness variation between 50 and 70 µm) and an inner Ni layer (100µm).

A few small porosities could be observed locally at the Ni/steel interface, which indicates a good quality of the Ni deposition process. From the thermodynamic point of view, any stable phase at 650^{o}C within the Al-Ni binary phase diagram can form during the coating preparation process. In practice, however, kinetics play a large role and only Ni_2Al_3 was observed directly after the low temperature aluminizing process. The reason is that the interdiffusion coefficient for Ni_2Al_3 is at least two orders of magnitude higher than for the other nickel aluminides [32].

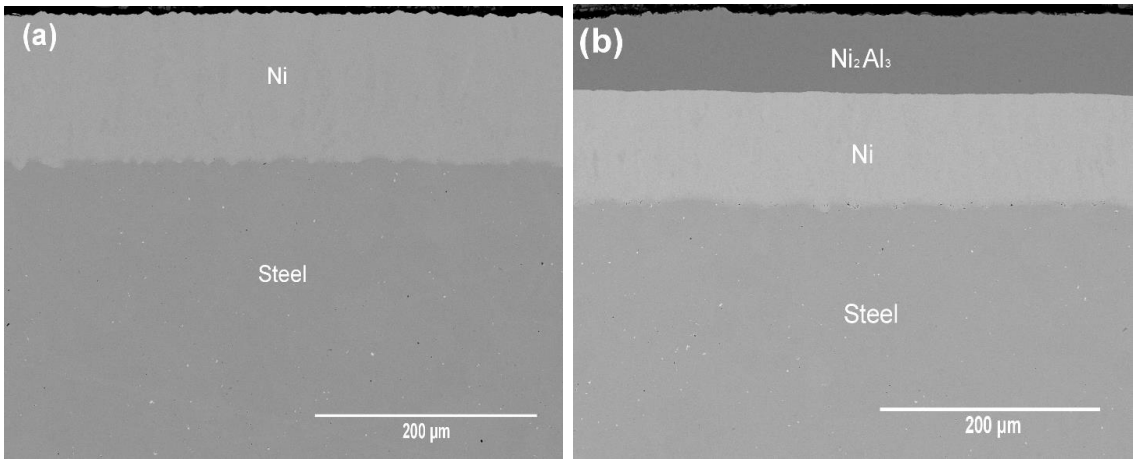

Figure 16. *BSE micrograph of the as coated samples for (a) Ni coated and (b) Ni_2Al_3 coated.*

1.5.7.3 Deposit analysis

The deposits were removed from the exposed tubes and examined with SEM-EDX. The deposit from Randers was sintered to the tube and a scalpel was required for removal whilst the deposit from MSK was fragile and easily flaked off. Photographs of the deposits are shown in Figure 17. The deposit from Randers was more compact with different layers where a whitish layer was present adjacent the tube. When the deposit was removed from the tube, almost no oxide was adherent. The deposit from MSK consisted of white crystals adherent to the underlying oxide and on the coated tube. Some of the coating was also present within the deposit.

The surface morphology and composition of the deposit close to the tube was investigated using SEM-EDX on both deposit flakes and cross-sectioned deposits. For deposit from Randers, the analysis of the underside of the deposit revealed two different morphologies (Figure 18a), a smooth morphology, which was probably KCl as the measured mole ratio for K/Cl was 1:1, and small particles that were presumably sulphates of potassium and calcium. Analysis of the dry polished cross-sections of the deposit also detected K, S, Ca and O and K, Cl rich regions (Figure 18b). These elements were present throughout the deposit; however-there were more Si rich fly ash particles on the outer part of the deposit.

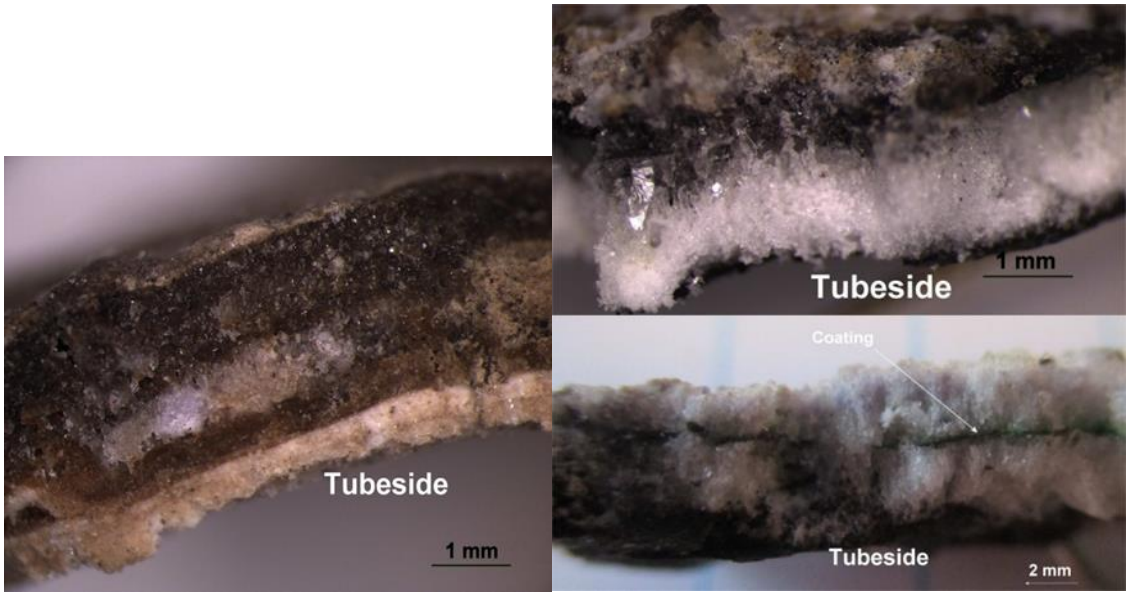

(a) Randers (b) MSK

Figure 17. *Appearance of deposits removed from the exposed tubes.*

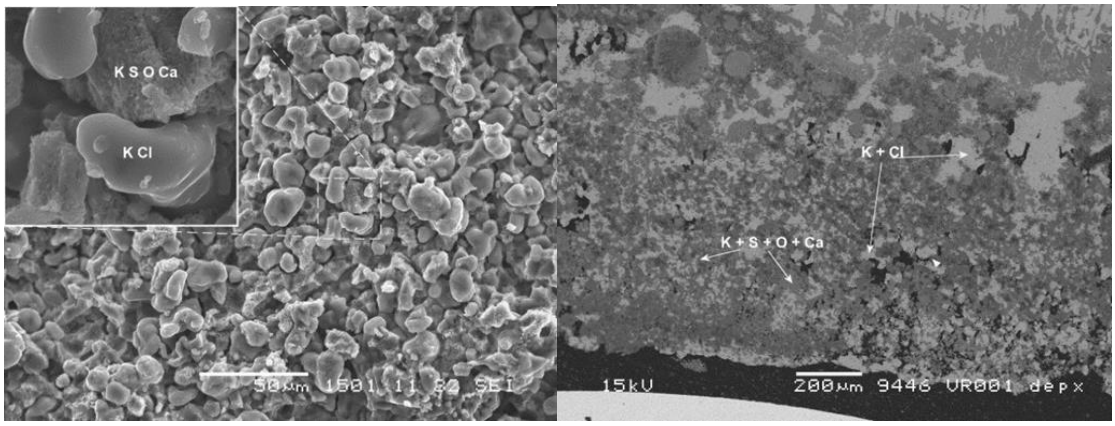

(a) Deposit adjacent the tube *(b) Cross section of the deposit*

Figure 18. *Surface morphology and composition of deposit from Randers*

Facetted cubic structures were typical on the unprepared deposit from MSK (Figure 19a), where the cubic structures had a composition corresponding to KCl. The KCl was in direct contact with the surface oxide and there were remnants of iron oxides on the surface. Cross sections of the dry polished deposit also showed that KCl is present adjacent to the oxide surface and there was only occasionally K, S, and O (presumably potassium sulphate) present (Figure 19b).

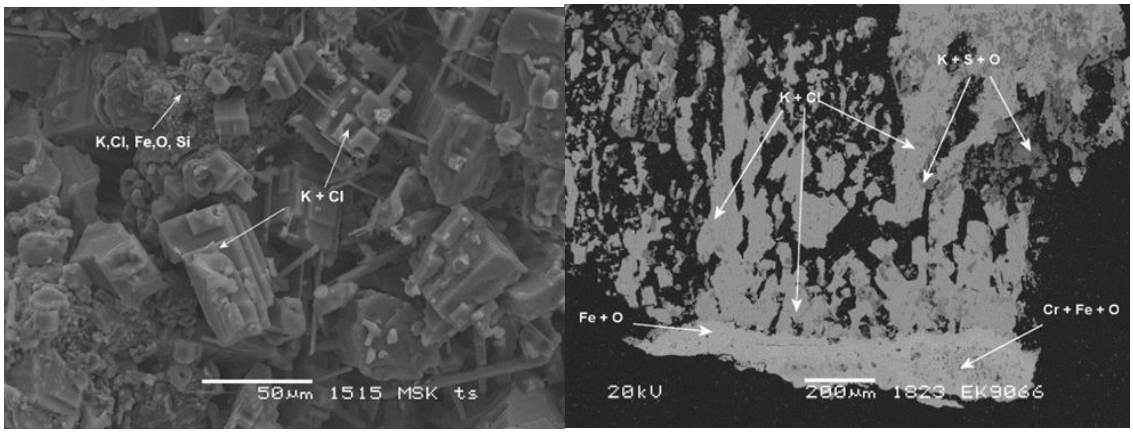

(a) Deposit adjacent the tube *(b) Cross section of the deposit*

Figure 19. *Surface morphology and composition of deposit from MSK.*

The high K and Cl content in the deposit adjacent the tube at MSK and Randers is due to the fuel used which was rich in potassium and chlorine. Since only small amounts of potassium sulphate were present adjacent the deposit at MSK, this would indicate that the sulphation process of KCl only has a partial contribution to the corrosion attack compared to Randers. In laboratory experiments, Okoro et al. [33] measured similar extents of internal corrosion attack for specimens in an oxidizing environment (CO_2+H_2O+O_2) with and without SO_2 + HCl, as long as KCl was present. The different morphologies of the KCl deposits may be linked to the tube temperature difference, which is lower at Randers than at MSK. Bröstrom et al. [34] investigated condensation of KCl and showed that above 500ºC, facetted KCl crystals were formed similar to Fig. 19a whereas at lower temperatures, a more dendritic appearance was apparent. They suggested that vapor is cooled by thermal condition from the metal tube, and then outward growth occurs by direction condensation of vapor phase to result in this structure.

At MSK, there were many thermal cycles and this could contribute to repeated spallation of the deposit resulting in new deposit forming on the tube. In contrast, the more sintered deposit from Randers may be more protective against incoming corrosive species. It could be suggested that after the initially formed KCl is exhausted, corrosion would decrease, as it would be more difficult for KCl to advance to the surface of the tube resulting in corrosion. Lindberg et al. [35] describes the behavior of a deposit due to a thermal gradient, revealing how deposit can be vaporized from the flue gas-deposit surface, and species can be trans-

ported and condensed throughout the underlying deposit, thus resulting in KCl being "transported" through a deposit with longer exposure times resulting in more KCl being transported. This would explain why KCl is present on the underside of the deposit. Cubic facetted KCl particles similar to those observed in the deposit from MSK were observed with TEM when SO_2 was not present in a gas stream in laboratory testing [36], otherwise KCl condenses on the potassium sulphate particles in the gas phase and then deposit on surfaces, which could be what has occurred at Randers.

During biomass combustion, potassium is present as KCl whilst sulphur is present as SO_2. When the temperature decreases below 1000ºC this will lead to oxidation of SO_2 to SO_3 and the sulphation of KCl to K_2SO_4, thus not only the presence of SO_2 but flue gas temperature will decide whether sulphation occurs [37]. With the limited information about the flue gas temperature and composition in the two different biomass fired plants, it is unclear whether the morphology of the KCl can be linked to the Cl:S ratio, the temperature gradient or other factors such as temperature changes. However the different morphologies and KCl abundance adjacent the tube reveals different environments around the tubes in the two plants which could have influence on the performance of the tested coatings.

1.5.7.4 Microscopy analysis of uncoated tubes after exposure

The corrosion morphology of the exposed uncoated tubes from Randers (Esshete 1250) and MSK (TP347H) after one year exposure are similar. The corrosion morphologies consist of a porous outer oxide, an inner selective corrosion area and grain boundary attack (Figure 20). The oxide located in the outermost corrosion product was rich in chromium and iron, while the oxide beneath was rich in nickel. No indications of formation of a protective chromium-rich oxide could be seen. This type of corrosion morphology is typical for chlorine induced corrosion, where volatile metal chlorides form via reaction with chlorine species. As the chlorine species are transported towards the outer surface they react with oxygen to form the porous outer oxide while the chlorine is released to again react and form new volatile metal chlorides, a chlorine corrosion cycle that is often referred to as active oxidation [2]. Because of the progression of the corrosion attack it is unclear if an initial breakdown of protective oxide scale occurred due to potassium chromate formation from a chemical reaction between chromium rich oxide and KCl as shown in laboratory studies [11, 34, 35] or whether corrosive chlorine species could enter into the steel along pores or cracks in the oxide.

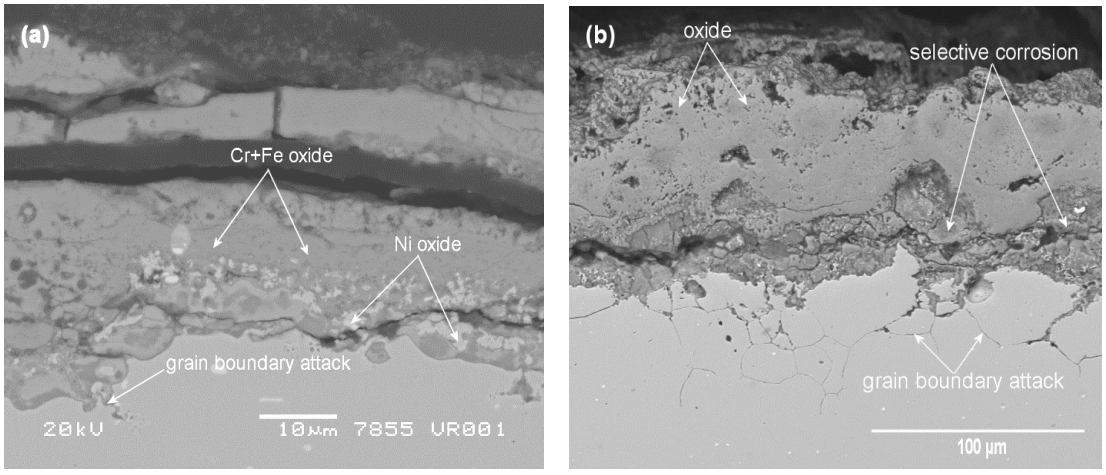

Figure 20. *Corrosion morphology on uncoated tubes after boiler exposure in (a) Randers and (b) MSK.*

After one year exposure, the actual metal loss for the non-coated steel was measured for both plants. The corrosion rate was then calculated based on the measured metal loss and the total exposure time (Table 5), which clearly reveals that the corrosion in the MSK plant is much more aggressive than at Randers. For the exposure in MSK, the average metal loss and corrosion rate are almost 30 times higher than Randers.

Table 5. *Average metal loss and corrosion rate for Randers and MSK*

Power plant	Randers	MSK
Average metal loss (μm)	23(±8)	651(±139)
Average corrosion rate (μm/1000h)	3	105

After two years exposure the metal loss of the uncoated tube from Randers was measured in 24 positions around the circumference of the tube (Figure 21). The position 12:00 marks the flue gas direction. The tubes after 2 years exposure exhibited more attack around the circumference compared to 1 year with an increased amount of grain boundary attack, but the maximum depth of attack did not increase.

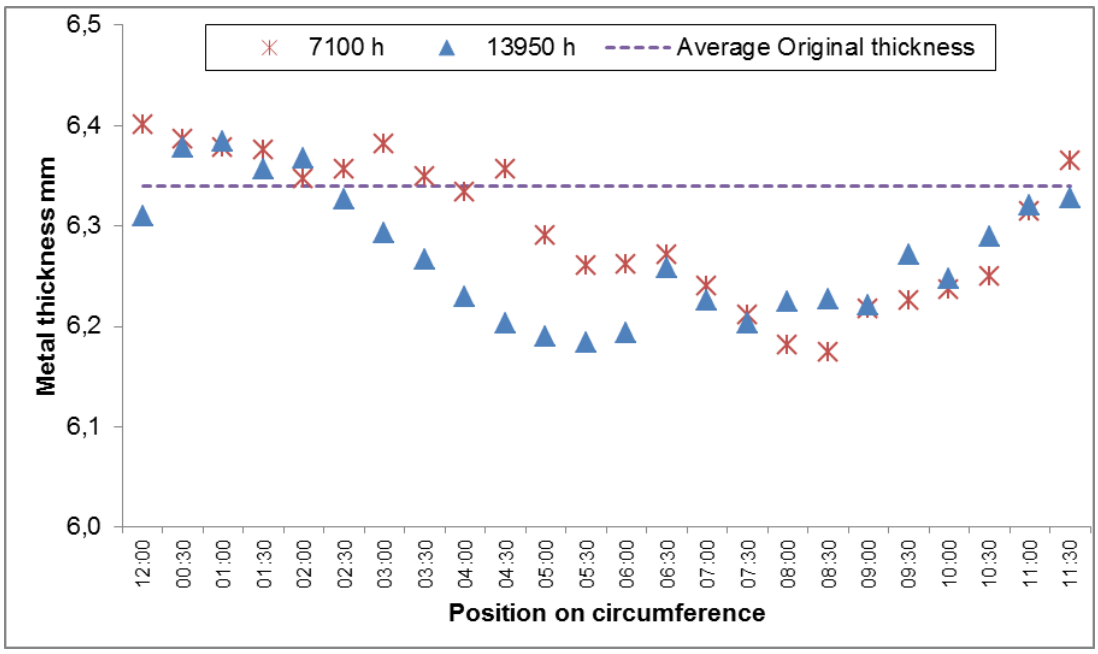

Figure 21 *Residual metal thickness of Esshete 1250 after 1 and 2 years exposure in Randers (red data points from 1 year exposure).*

Typical cross-sectional microstructure of the uncoated reference tubes from Randers after 1 year (2015-2016) and 2 years (2015-2017) boiler exposure are presented in Figure 22. The corrosion morphologies consisted of an outer Fe rich oxide and an inner more Cr rich oxide and Cr enrichment along the grain boundaries. A greater amount of grain boundary attack was observed after 2 years exposure.

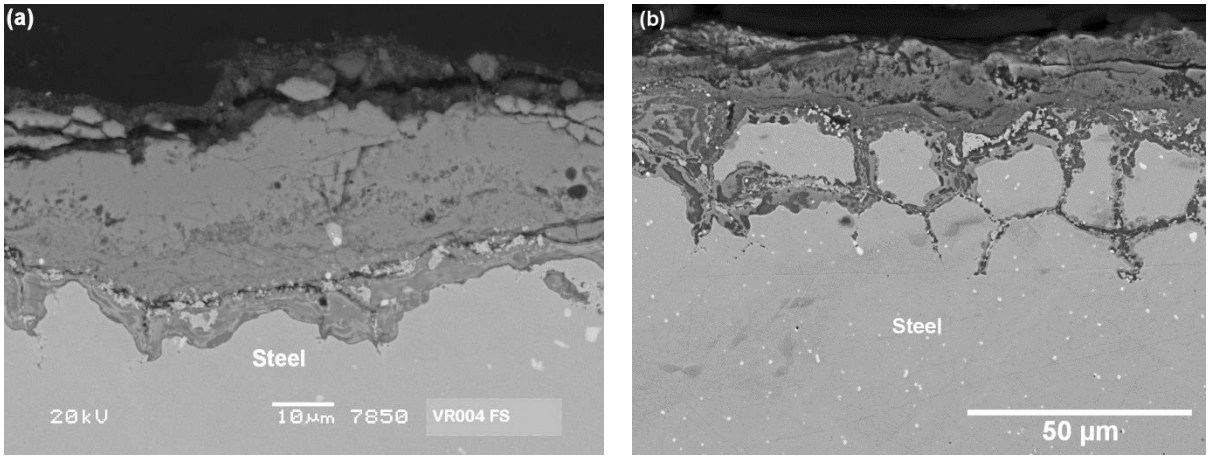

Figure 22. *Back-scattered SEM micrographs of cross-sections of the uncoated Esshete 1250 reference tubes, (a) 1 year boiler exposure, (b) 2 years exposure.*

1.5.7.5 Microscopy analysis of Ni coated tubes

The corrosion morphology of the exposed Ni coated tubes for Randers and MSK are very different as shown in Figure 23. The Ni coated tube showed good performance after exposure in Randers where the Ni layer was still attached to the steel and no significant attack was measured. The measured metal loss is 3.37(±2.25) µm and the calculated corrosion rate for Ni is 0.47 µm/1000h. Similar results have been observed in the laboratory. Ni revealed a significantly better performance compared to Fe-Cr-Al alloys at 670ºC with KCl in air, but had lower performance compared to NiAl alloys [14]. When two different exposures were conducted at 600ºC with slightly different oxidising gases and with and without KCl, a nickel oxide of 4 µm was formed in both exposures even though the amount of KCl was much higher in one of the experiments [11]. However, for the exposure in MSK, severe attack occurred and the 135µm Ni layer was no longer present. The corroded tube section had a mixed iron and chromium oxide at the surface and grain boundary attack into the substrate steel, which was similar to the corrosion morphology observed on the uncoated tube. It is highly probable that the slight mismatch in thermal expansion coefficients (Fig 31) gives problems where there is excessive thermal cycling at MSK. Thus cracks/channels can form that allow for the migration of corrosive species to the Ni-steel interface and the outward migration of Cr chlorides. The corrosion attack thus occurring underneath the Ni-layer will further contribute to poor adhesion between Ni-layer and steel tube.

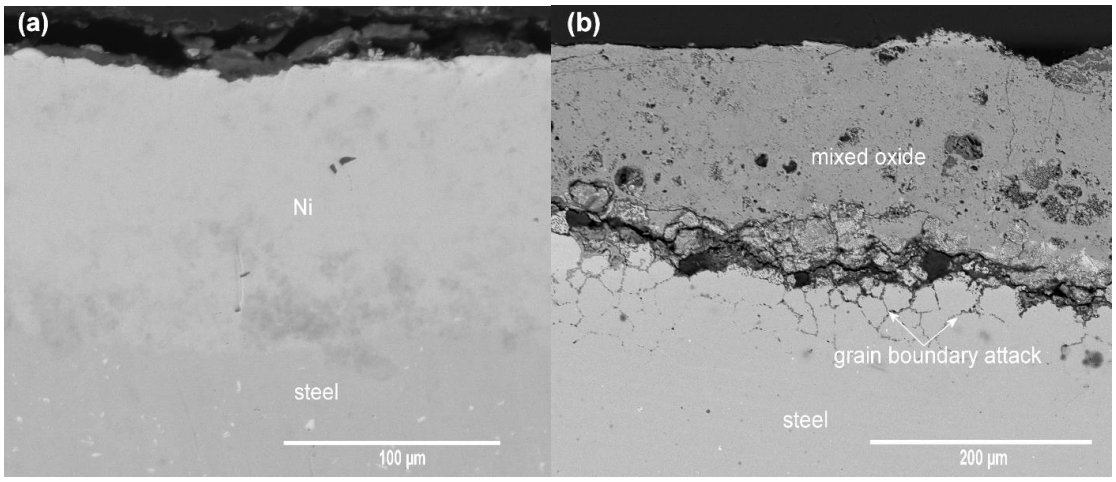

Figure 23. *Corrosion morphology on Ni coated tubes after boiler exposure in (a) Randers and (b) MSK*

The measured nickel coating thickness at Randers at 12 positions around the circumference is shown in figure 24. Since the initial nickel layer was about 135µm, and after the 1st year the average thickness was 133±4µm, there was minimal removal of the nickel layer, however after the second year, there was a clear decrease in thickness on the flue gas side and the leeside. The cross-sectional microstructures of the Ni coated tubes after exposure in the power plant are shown in Figure 5. Compared with the 1 year exposure, a much thicker Ni oxide had formed on the coating surface after 2 years exposure. After the second year the Ni coating was still well adherent to the underlying substrate and the substrate was apparently protected. No cracking was identified within the Ni coatings, however the presence of very small "precipitates" (at a depth shown by the double headed arrow) was observed only for the tube exposed for 2 years. These precipitates were clearly visible at higher magnifications (Figure26).

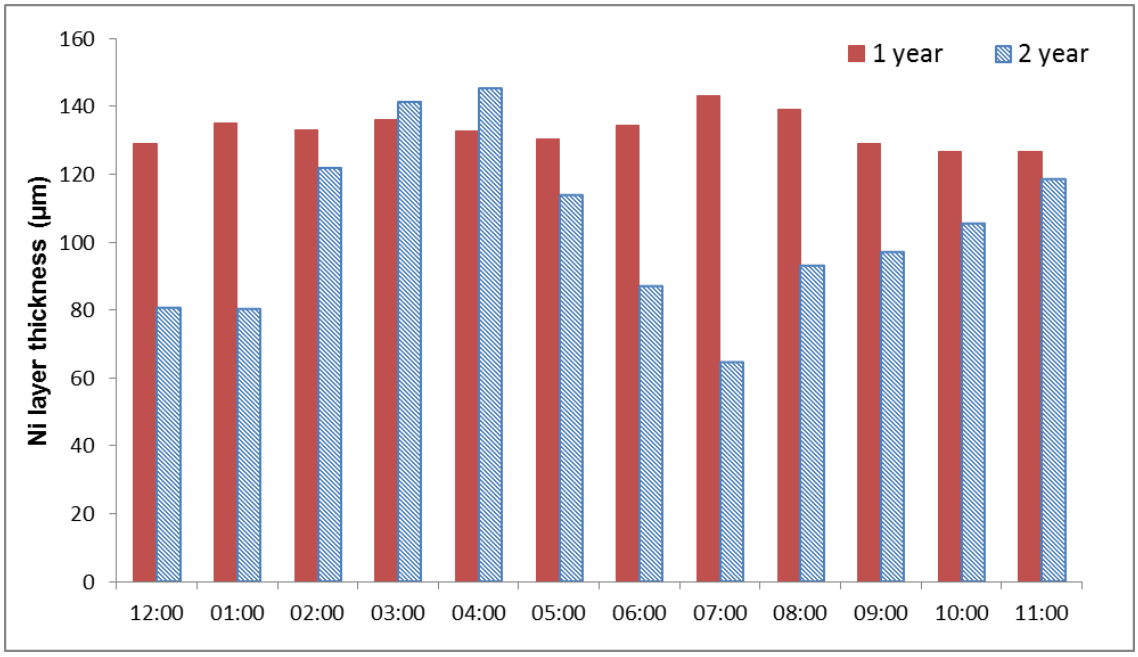

Figure 24: *Comparison of Ni layer thickness after exposure for 1 and 2 years at Randers.*

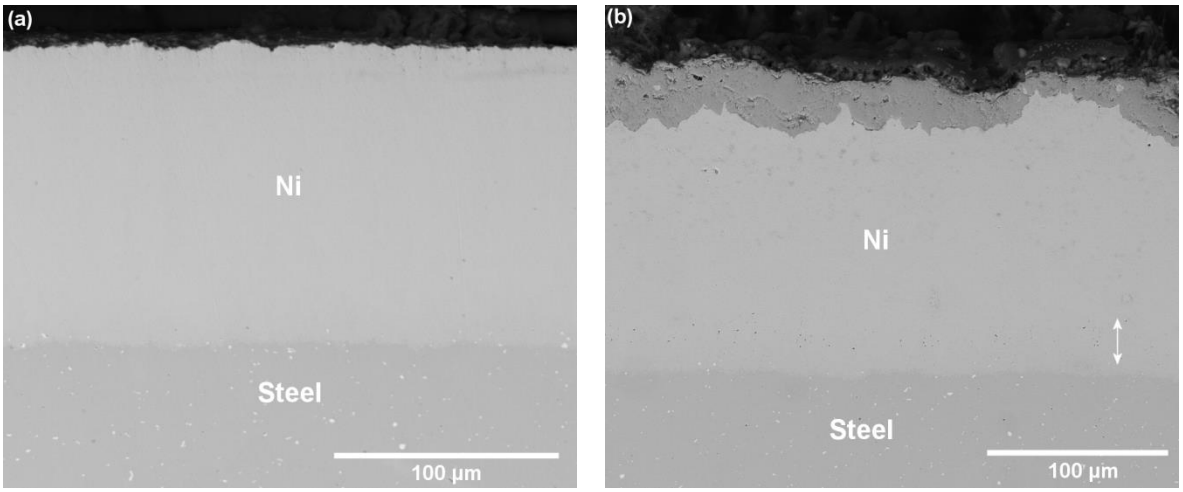

Figure 25: *Back-scattered SEM micrographs of cross-sections of the Ni coated tubes, (a) 1 year exposure, and (b) 2 years exposure.*

Further examination of the Ni coating near to the nickel-stainless steel interface revealed that there were enrichments of Mn and S at grain boundaries in the Ni layer shown by the arrow (Figure 26a). For the precipitates shown in Figure 26b, some of the surrounding area was also analysed due to the SEM-EDX interaction volume of the analysis, however the indication of sulphur and increased Mn was clear. The measured Mn contents were 5 wt.% which is significantly higher than the 1 wt.% Mn that was measured in the general interdiffusion area next to the precipitates. The Mn+S enrichments were always present within the nickel layer above the nickel-steel interface, probably at grain boundaries. Pathways from the nickel oxide surface through the Ni-layer could occasionally be observed; however in many cases they were not as evident as in Figure 26a. Careful re-examination of the tube cross-sections from one year exposure revealed almost no Mn and S enrichments, indicating that their formation primarily occurred during the second year.

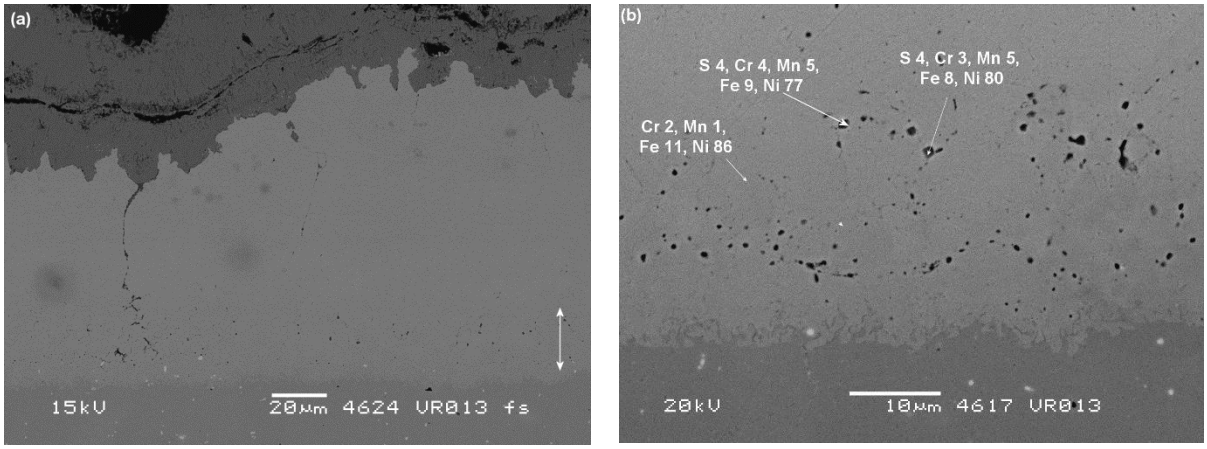

Figure 26: *Other areas of tube after 2 years exposure a) showing intergranular pathways from oxide and region of precipitates (white double headed arrow), b) higher magnification at the alloy-nickel interface revealing Mn+S rich precipitates with analysis in wt.%.*

1.5.7.6 Microscopy analysis of Ni_2Al_3 coated tubes

- *Exposure in Randers*

The coating thickness was measured after exposure in 12 positions clockwise around the circumference of the Ni_2Al_3 coated tube as shown in Figure 27 where 12:00 is the flue gas direction. The coating thickness around the Ni_2Al_3 coated tube is asymmetric. The deposit growth is typically asymmetric around a superheater tube depending on the flue gas flow conditions that vary around the tube. The attack at areas opposite the flue gas may be due to the varying deposit parameters on the upstream (12:00) compared with the downstream (06:00) part of the tube [38].

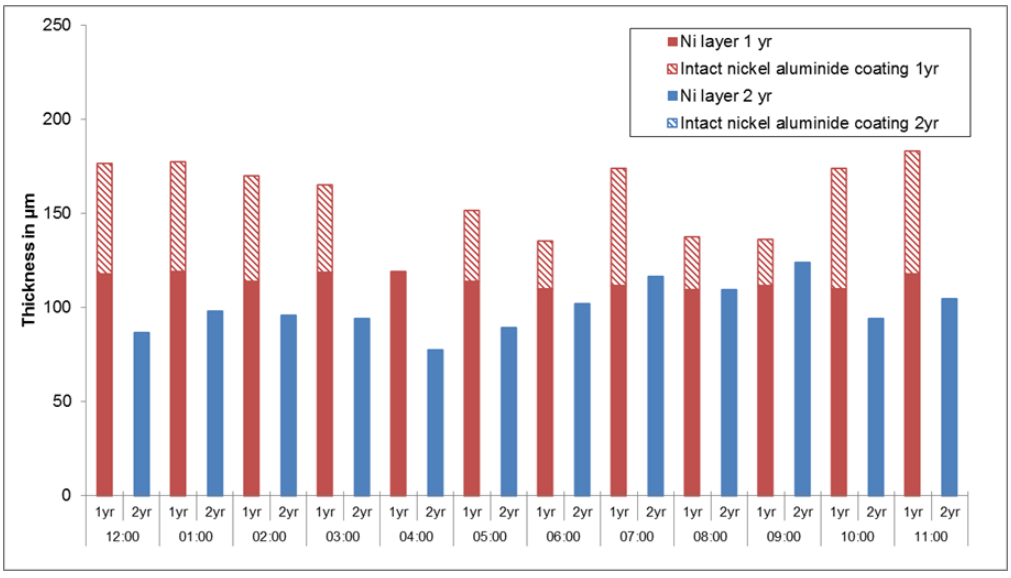

Figure 27. *Residual thickness of layers around the circumference of the Ni_2Al_3 coated tube in Randers.*

After 1 year exposure, the nickel aluminide coatings were still present in most positions and only in one position had the coating spalled. In several positions, the nickel aluminide coating was attacked and the attacked part of the coating was converted into corrosion products. After the first year, the underlying Ni layers (with thickness around 110-125 µm) were still attached to the underlying substrate and were not attacked in any of the positions. After 2 years exposure, the nickel aluminide coatings were severely depleted and intact nickel aluminide coatings (diagonal pattern on bar chart) were no longer present. The Ni layer was still adherent to the tube and only slightly attacked at the nickel aluminide coating-Ni interface where the lowest measured Ni thickness was 77µm.

In Figure 28, the typical morphology of corrosion products observed on the nickel aluminide coated tubes after corrosion exposure in the biomass boiler for 2 years is shown. Figure 28a shows a spalled nickel aluminide coating, which corresponds to position 3:00 in figure 27. The corrosion attack had completely consumed the coating and it had then spalled at the coating-Ni interface. For most of the area around the circumference (~90%), Figure28b is a representative micrograph where the nickel aluminide coating was attacked and where corrosion products containing aluminium were still adherent. The composition and the distribution of the corrosion products in Figure 28b is presented in the elemental distribution maps. In this area, the outer layer consisted of K, S and O, presumably K_2SO_4 from the deposit, however the deposit analysis indicated that more KCl was present in other areas. Below the deposit, a porous corrosion product containing Al and Ni was identified with O and K also present within this layer. Traces of Cl were observed at the surface of the deposit probably as KCl and at the corrosion front at the left hand side of the micrograph. There were some Ni rich regions within the corrosion product which were analysed to be unreacted metallic Ni.

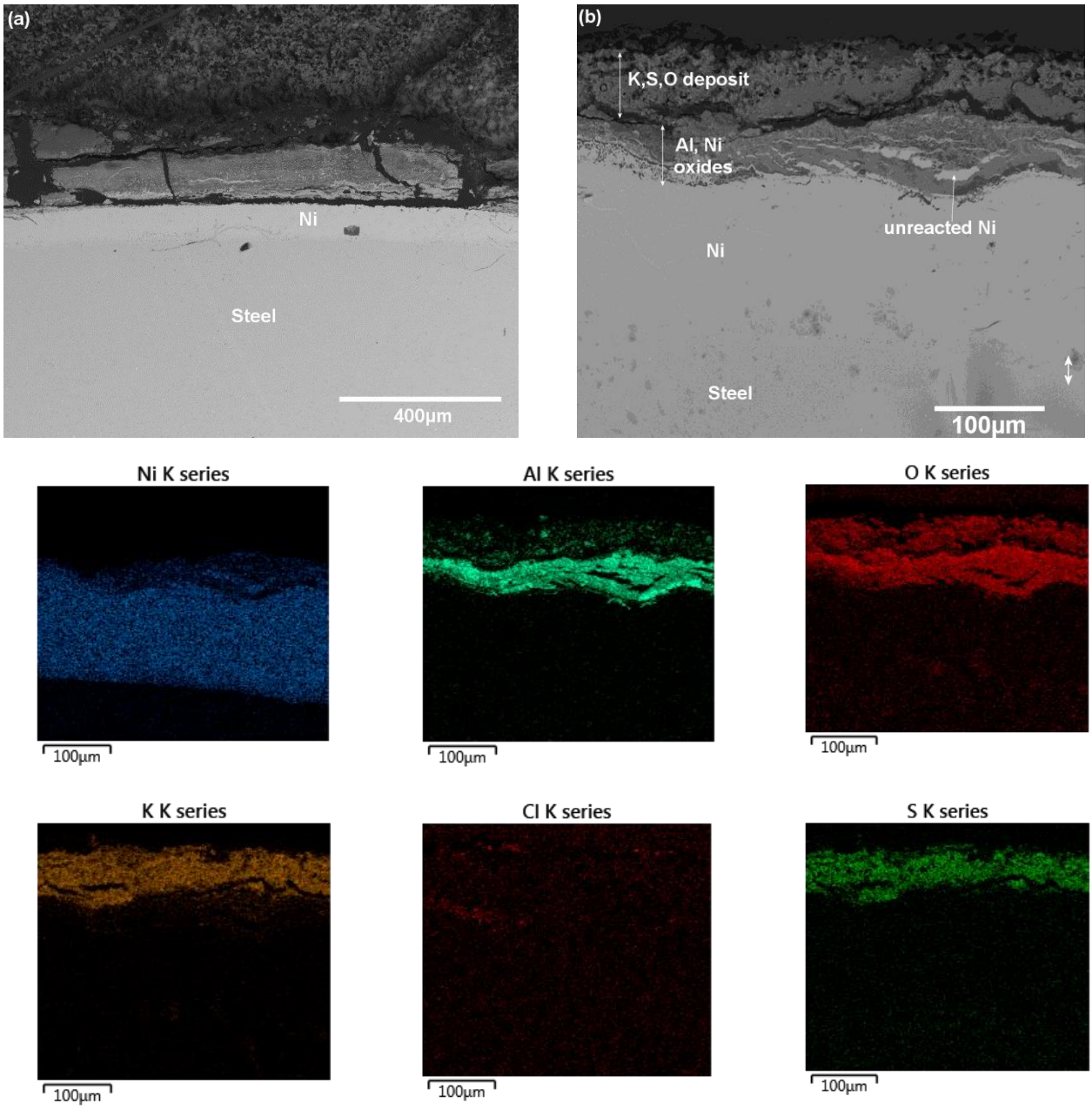

Figure 28: *Back-scattered SEM micrographs of cross-sections of the nickel aluminide coated tubes after 2 years boiler exposure in Randers, (a) spallation of the nickel aluminide coating, (b) corrosion attack of the nickel aluminide coating revealed by EDS mapping.*

To understand the degradation leading to the complete failure of the nickel aluminide coating after the second year, different stages of local corrosion attack of the nickel aluminide coating after the first year were studied in detail with SEM. Figure 29 shows localized areas after the first exposure year with different degrees of attack ranging from very limited attack in Figure 29a to descaling of the coating shown in Figure 29d. At most locations the nickel aluminide coating exhibited the behavior shown in Figure 29a with only slight surface attack, which corresponds to the positions on the tube circumference from 10-3 o'clock and at 7 o'clock. In the positions shown in Figure 29b-d the coating was attacked and aluminium depletion of the coating was visible. The worst case location corresponding to the 4o'clock position is shown in Figure 29d, where the nickel aluminide coating reached end of life, and the underlying Ni layer was being attacked. At all locations, the underlying steel was still well protected without sign of corrosion attack.

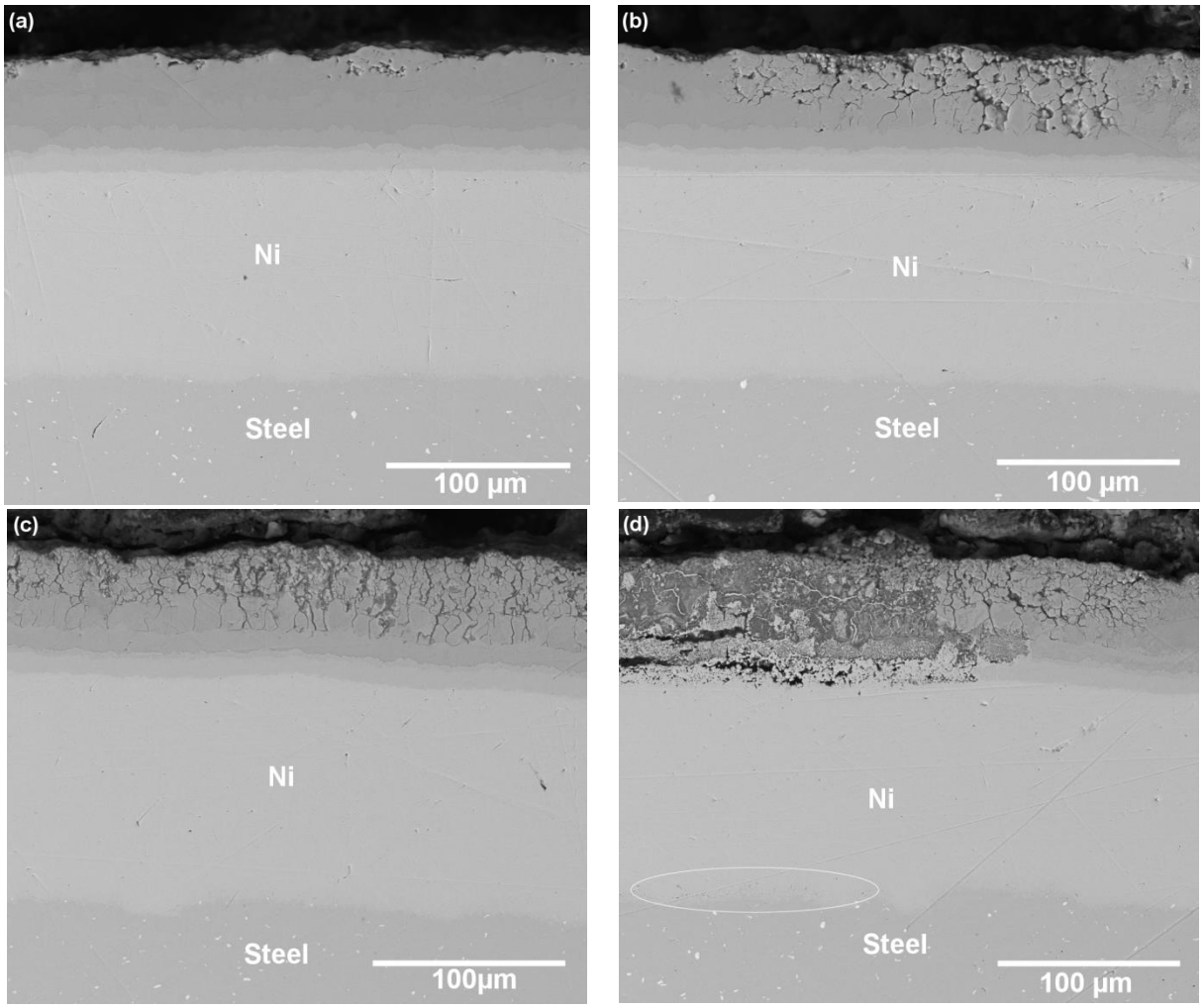

Figure 29: *Back-scattered SEM micrographs of cross-sections of the Ni_2Al_3 coated tubes showing different corrosion stages after 1 year boiler exposure, (a) protective surface, (b) Al depletion and porosity formation,(c) porosity and corrosion propagation, (d) penetration attack and coating spallation (white ellipse showing position of internal precipitation).*

Compared with Ni, Fe and Cr, Al has the highest affinity for reaction with both chlorine and oxygen. Presumably, aluminium chloride can form at the deposit/Ni_2Al_3 coating interface when the oxide partial pressure is low. Because of the low melting point of aluminium chloride (192 ^{o}C), aluminium chloride will volatilize and migrate outwards rapidly. The volatilized aluminium chloride will be transformed into aluminium oxide where the oxygen partial pressure is higher, leaving behind a depleted or porous area. Li et al. [14] saw rapid early stage volatilization when exposing Fe-Al alloys and a NiAl alloy to NaCl-KCl melts at 670 ^{o}C but observed that the attack slowed down when a thicker alumina layer was established on the surface. This agrees well with the corrosion morphology observed on the Ni_2Al_3 coated tube in Figure 29a. The surface attack of the Ni_2Al_3 coating indicates that an initial corrosion attack has happened, while a continued attack did not occur. However, in some locations (localized attack in Figure 29b) there was no slowing down when attack was initiated. Some

studies have argued that this type of attack can be due to a chemical reaction between alumina and gaseous KCl where the flue gas temperature is high, which can break down the protective alumina [12]. According to the investigations by Pettersson et al. [39], gradual volatilization of KCl would occur at temperatures above 560°C, where the vapor pressure of KCl exceeds 10^{-6} atm. With the breakdown of the protective Al_2O_3, the corrosion process could proceed and a porous Al-depleted layer would develop underneath the surface (Figure 29b).

- *Exposure in MSK*

Compared with the exposure in Randers, the Ni_2Al_3 coated tube performed much worse in MSK. As shown in Figure 30, the nickel aluminide layer was no longer adherent to the tube; this was the case around the whole tube circumference. The spalled nickel aluminide coating could be found within the deposit, and investigations showed that in the spalled section some Al depletion had occurred but there was still alumina. Remnants of an oxidized nickel layer (up to 70 µm) were present in approximately two-thirds of the circumference of the tube sample with varying depths of attack of the underlying tube. This indicates that the Ni_2Al_3 layer offered some initial protection before spalling off, since there was no Ni left on the tube coated only with Ni (cf. Fig. 23b). The presence of a Ni_2Al_3 coating hinders evaporation of metal chlorides from the corrosion front, but does not prevent Cl species diffusing to the corrosion front. Beneath the Ni layer, the formation of trapped nickel chloride also hampered the corrosion process by binding the aggressive chlorine.

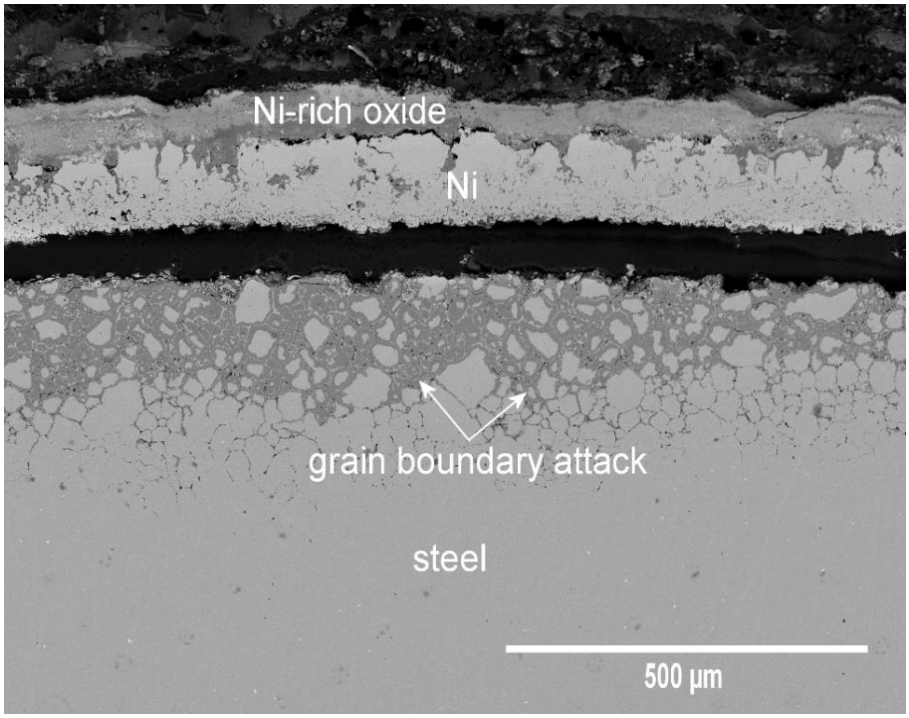

Figure 30. *BSE image of corrosion morphology for the Ni_2Al_3 coated tube after boiler exposure in MSK*

Since there are many thermal cycles at MSK (Figure 9), the most probable explanation for the spallation of the Ni_2Al_3 coating lies in the difference in thermal expansion coefficients between the steel, Ni, Ni-Al intermetallics forming at the interface and the Ni_2Al_3. The coefficients of thermal expansion (CTE) for the steels, Ni, NiAl and Ni_2Al_3 are depicted in Figure 24. For the power plant exposure temperature interval between 300°C and 600°C the CTE for Ni_2Al_3 differs significantly from the CTE for Ni, NiAl and steels. A full stress analysis is outside of the scope of the present work, however, as the CTE for Ni_2Al_3 and Ni are quite different, thermal stresses could be expected which would lead to the spallation of the Ni_2Al_3 coating in MSK. The spallation of Ni from the steel was probably related to the corrosion attack of the underlying steel which led to a weak adhesion between Ni and steel.

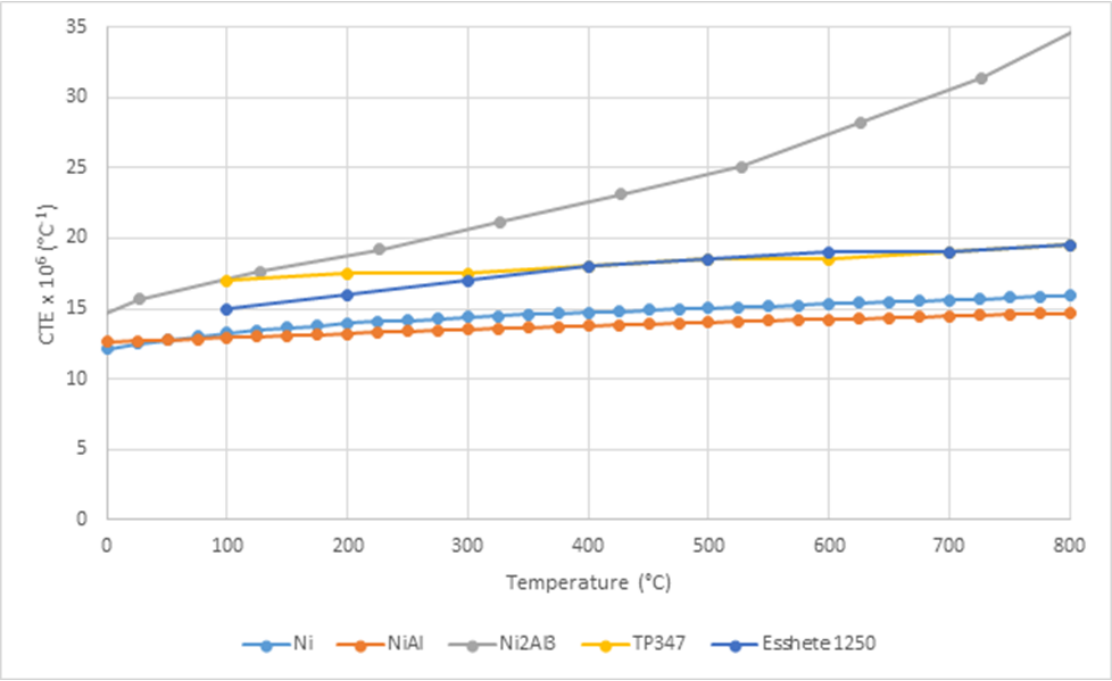

Figure 31. *The variation of CTE with temperature of pure Ni, NiAl, Ni_2Al_3, TP347H and Esshete 1250 [40,41]*

1.5.7.7 Investigations of tubes with amended coating systems

The coatings selected for year two exposure based on laboratory results showed in general similar performance as the Ni and Ni_2Al_3 coated tubes [27]:

- The preoxidized and CeO_2-dispersed Ni_2Al_3 coatings showed similar corrosion behavior as the normal Ni2Al3 coatings after exposure in a wood firing power plant with an outlet steam temperature of 520^{o}C for 6850 h.
- For preoxidized and CeO_2-dispersed Ni_2Al_3 coatings, the enrichment of K, Al and O was identified in the corrosion front and no chlorides were observed after boiler exposure.
- The nitride coating slowed down the corrosion attack in some areas with Fe-rich oxide formed on the outer surface. In other areas, the boiler exposure resulted in grain boundary attack of the steel and selective attack of Cr was observed.

In conclusion, no significant improvement was achieved by the amended coating system. Thus, the general discussion of plant exposure addresses only the Ni and Ni_2Al_3 coatings.

1.5.7.8 Comparison of coating performance depending on plant

Based on the above discussions the applied Ni and Ni_2Al_3 coatings show very different corrosion performance in the different biomass fired power plants. In the Randers plant, both the Ni and Ni_2Al_3 coatings showed protective behaviour, while the coatings spalled off when exposed in MSK. The fuel utilized, operation temperatures and temperature cycling characteristics differ hugely between the two plants as do the corrosion rates. These are critical factors that play a key role in the observed coating performance.

- *Fuel comparison*

According to Table 4, there are clear differences between the fuel data for the two plants, Randers and MSK. Most important is that the content of potassium and chlorine in MSK is much higher than in Randers. It is widely accepted that fireside corrosion is mainly induced by a high content of potassium and chlorine from the biomass fuel [42]. Besides the content of potassium and chlorine, the sulphur to chlorine ratio also plays an important role for superheater corrosion [43,44]. The investigation by Krause et al. [44] showed that the corrosion problem is significantly reduced when the sulphur to chlorine mole ratio (S/Cl) in biomass fuel is high i.e. 4. Grabke et al. also reported a similar tendency in their study [43]. It has been suggested that the best way to prevent corrosion during biomass firing is to keep

the S/Cl ratio in the fuel higher than 2.0 and preferably higher than 4.0 [45]. For our exposure studies, the S/Cl ratio in Randers was 1, while in MSK it was 0.76 so that corrosion due to KCl would be expected in both cases. The differences in S/Cl ratio are consistent with the analysis of the deposits. Larger amounts of potassium sulphate were present within the deposit adjacent the tubes in Randers than in MSK. The sulphation process of deposited KCl can also affect the corrosion attack; the sulphation of potassium chloride to potassium sulphate with the release of a high partial pressure of chlorine can take place both at the oxide-deposit interface and near the deposit surface [46]. Most of the released chlorine will diffuse into the atmosphere, whereas a fraction diffuses inward resulting in corrosion [42]. However the presence of KCl in oxidising environments (O_2+H_2O+O_2) without SO_2 can result in similar corrosion attack, as KCl can also react directly with oxides to release corrosive Cl species [47,48].

- *Temperature data comparison*

The temperature data during the exposure period from Randers and MSK (Figures 8-10) show significant differences. The average test tube steam outlet temperature in Randers was 512 °C, while in MSK it was 544 °C. The significantly higher average steam temperature at MSK than at Randers would obviously increase the degree of fireside corrosion. Randers also has a broader temperature range with a significant amount of hours below 500ºC where there would be minimal corrosion for an austenitic steel. As has been previously observed for these types of steels, corrosion increases significantly with increase in temperature [49] and this is probably the main reason for the higher corrosion rates of the steel tubes observed for the MSK plant. Another important factor is the thermal cycling of the plants. The plant in Randers has only had one shutdown during the entire exposure period and otherwise the operation temperature has been relative stable. This is in complete contrast to the MSK plant where frequent thermal cycling resulted in severe exposure conditions. At the MSK plant there has been three full shutdowns, but during autumn and late spring, there was thermal cycling every day between 200 and 540 °C (Figure 9) resulting in 213 start/stop cycles (Table 3). This is with high certainty the reason behind the spallation of both Ni and Ni_2Al_3 coatings in the MSK boiler.

1.5.7.9 Overall conclusion of in-plant tests

The present work shows that the performance of the coatings is related to the specific operation conditions of the different plants. For the MSK plant, the frequent temperature cycling is a huge challenge for any coating. A very close fit in thermal expansion coefficients between steel and coating would be necessary for any coating to survive in this condition.

For the Randers plant, this is of less importance since almost no cycling is carried out, which implies that this type of plant is a more obvious candidate for life time extension through coating application. The initial results after 1 year were positive for both the Ni coating and the nickel aluminide coating. However, despite the low temperatures in this boiler, the Ni coating was attacked after two years and revealed intergranular attack and formation of metal sulphides.

The nickel aluminide coating was completely consumed after two years through chemical degradation and subsequent descaling. The exposure in the plant has highlighted chemical mechanisms of degradation which were not apparent from short-term laboratory exposures. The fact that there were differences from 1 to 2 years highlights the necessity for long-term plant exposures.

1.5.8 Feasibility study

The idea behind the present project is that coatings with superior corrosion resistance compared to uncoated tubes can be used to increase live steam temperatures and thereby efficiency of the power plants, without compromising availability and maintenance costs.

The coated tubes subjected to real operating conditions in the present project, unfortunately showed that the tested coatings did not provide the desired protection against Cl induced corrosion in biomass fired boilers. It is however still relevant to investigate the potential benefits of new coatings or materials solutions with superior corrosion resistance compared to the current best available technology of 18%Cr austenitic steels.

In the following the theoretical economic benefits are estimated based on case studies of both CHP plant types, taking into consideration the increased efficiency as well as maintenance and fabrication costs.

1.5.8.1 Increased steam cycle efficiency

Two cases will be used to illustrate the economic benefits of increased power plant efficiency, achieved by higher steam temperatures than 540°C:

Case 1: New local biomass unit with 120MW heat input, live steam temperature of 560°C and electrical and total efficiency of. $\eta_{el} = 0.32, \eta_{tot} = 0.9$

Case 2: Existing central coal fired CHP plant with 800MW heat input converted to biomass and live steam temperature reduced from 580°C to 540°C. The efficiency before conversion is $\eta_{el} = 0.45, \eta_{tot} = 0.7$

Case 1 is chosen to illustrate a biomass CHP plant at a size typically built today e.g. like Verdo in Randers. Case 2 is chosen to illustrate large CHP plants with high efficiency like e.g. Nordjyllandsværket in northern Denmark, if converted from coal to biomass.

To estimate how the temperature affects the power plant efficiency, the theoretical Carnot efficiency is used. When the cold reservoir temperature is held constant at 40°C (typical district heating return temperature), the Carnot efficiency as a function of live steam temperature is as presented in figure 32. This gives the theoretical improvement in mechanical efficiency which is assumed to be the same as the overall plant efficiency. Due to component loses etc., as a conservative approximation it is assumed that maximum half of the Carnot efficiency improvement can be achieved with the real steam cycle.

As illustrated in figure 32, the changes in live steam temperature in both the cases give rise to potential efficiency changes:

Case 1: An increase in live steam temperature by 20K (540° to 560°C) theoretically increases the efficiency 0.9%. It is assumed that half of this (0.45%) can be realised in the actual steam cycle

Case 2: A decrease in live steam temperature by 40K (580° to 540°C) theoretically decreases the efficiency 1.8%. It is assumed that half of this (0.9%) is lost in the actual steam cycle

To verify that the Carnot efficiency is a good approximation for the efficiency change of the actual steam cycle, simulations were made in a thermodynamic model of a steam cycle much like the one in Nordjyllandsværket (case 2). The steam cycle is illustrated in figure 33. Two simulations were made, one at the design live steam temperature of 580°C and one at a steam temperature (main and reheat) reduced to 540°C, simulating before and after conversion to biomass. The simulation results are presented in Table 6. As shown the total efficiency decreases with 1.23% when the steam temperature is reduced with 40°C. The approximation of 0.9% for a 40°C decrease based on the Carnot efficiency therefore seems reasonable yet conservative.

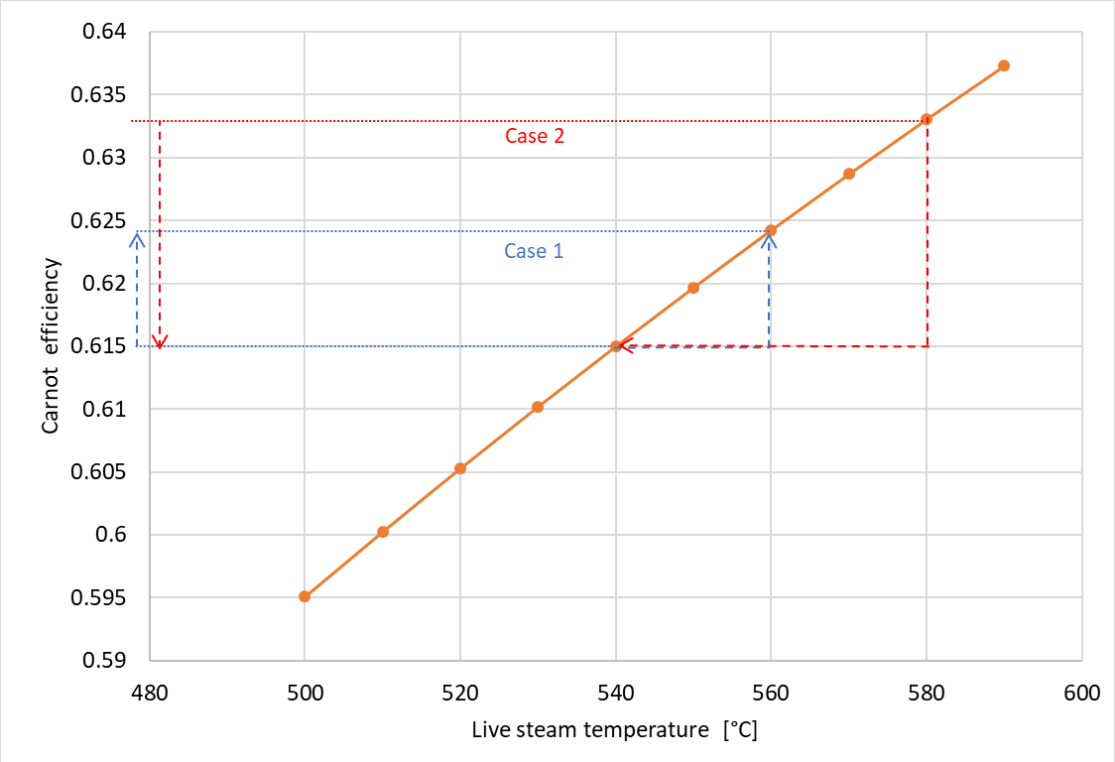

Figure 31: *Carnot efficiency as a function of live steam temperature. The cold reservoir temperature is held constant at 40°C which is the typical district heating return temperature determining the pressure sink.*

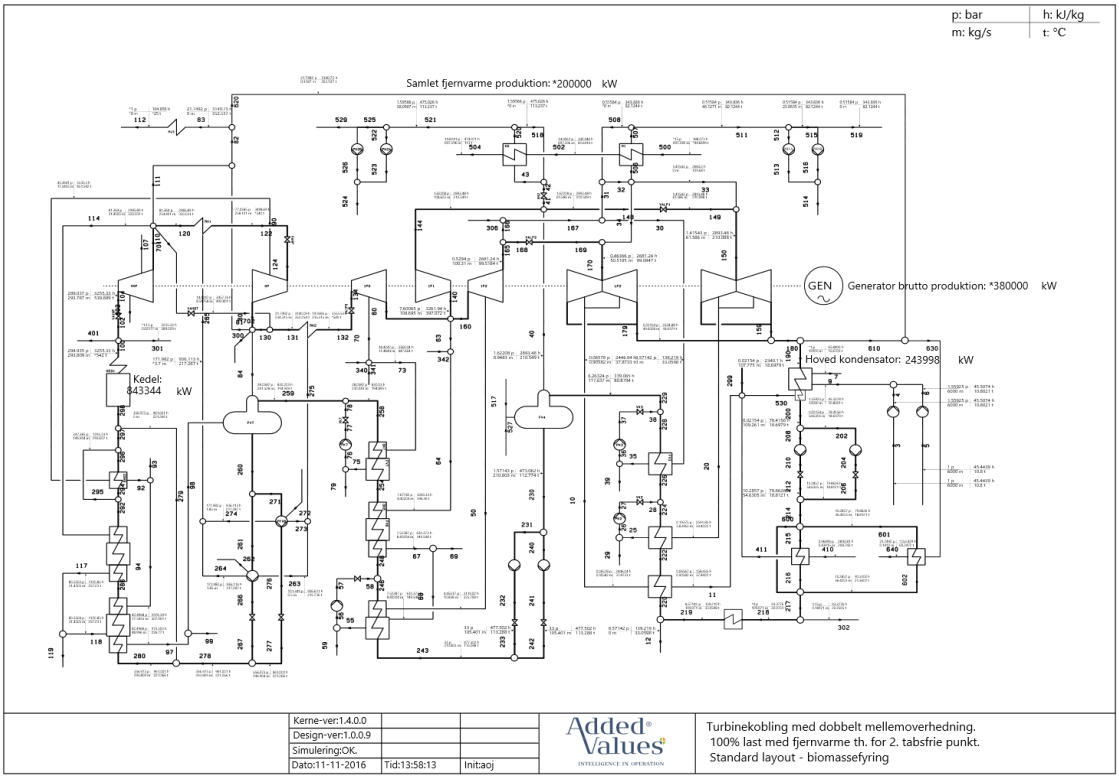

Figure 32: *Steam cycle of central CHP plant with double reheat.*

Table 6: *Calculated change in efficiency after conversion to biomass with reduced steam temperature for the steam cycle presented in Figure 32.*

	After	Before	Change	Unit
Steam temperature	540	580	40.00	[°C]
Pel	380	380	0.00	[MW]
Qfjv	200	200	0.00	[MW]
Qked	843	829	-14.84	[MW]
mked	294	273	-20.79	[kg/s]
nyel	45.06	45.87	0.81	[%]
nyq	23.72	24.14	0.42	[%]
nytotal	68.77	70.01	1.23	[%]

The potential savings in fuel consumption over the plant lifetime (200,000h) under the assumption of constant heat and power output can then be computed. The results are presented in table 7. Most plant owners would probably choose to increase the heat and power output rather than reduce fuel input, leading to increased earnings from sales. For simplicity, given the high volatility of heat and power sales and the price differences across European markets, it is chosen to fix the heat and power output and look at potential fuel savings. For case 1 it is also assumed that the higher steam temperature can be achieved without additional heat input (e.g. by reduced spray attemperation).

Table 7: *calculation of potential lifetime fuel savings with increased or maintained live steam temperature.*

	Case 1	**Case 2**
Lifetime [h]/[years]	200,000/25	200,000/25
Fuel	Wood chip	Wood pellets
Fuel price forecast ENS:2017[1]. Assumed 8000h/year		
Nominal heat input [MW]	120	800
Efficiency improvement [%]	0.45	0.9
Potential lifetime savings on fuel [Mkr]	20	355

1.5.8.2 Fabrication and repair methods

Compared with uncoated tubes, coated superheater tubes have some obvious challenges regarding fabrication and repair procedures, as welding compromises the corrosion properties of the coating. In the following sections, possible solutions to these challenges are presented.

Depending on the design and size of superheaters for biomass fired boilers, the fabrication process usually includes several butt welds. As the coating would be destroyed by the welding process, the coating must be done after welding. This can be done in two ways, either by coating the entire tube section after all welding has been finished, or by local coating of the welds. Coating techniques for both options are commercially available, e.g. pack cementation or slurry coating can be used for complex tube sections and thermal spraying could be used for local coating of the welds.

An alternative solution would be only to use coated tubes for the high temperature section of the superheater, and then use uncoated and even lower grade steels for the inlet part of the superheater. This would reduce the need for butt welds in the highly corrosive parts of the superheater. This sectioned design philosophy using cheaper steel grades in colder sections, has been used for many years in conventional coal fired power plants to reduce material costs. Using this solution would reduce the overall cost of the superheater and reduce maintenance costs as only shorter coated tube lengths would need to be replaced in repair situations.

[1] ENS = Danish energy agency. Produce yearly forecast on fuel prices. The forecast generally follow IEA.

In figure 34 the outside tube metal temperature as a function of distance from SH inlet of the Verdo final superheater is shown for a steam outlet temperature of 540° and 560° respectively. The calculations were performed in a numeric tube model with inlet/outlet steam temperature, steam pressure, steam mass flow, geometry and heat flux profile as inputs [31]. At the current maximum steam outlet temperature of 540°, the maximum outside metal temperature of 548°C is reached at 20m from the inlet. The same metal temperature is reached at 16.5 m with a steam outlet temperature of 560°C. Flue gas corrosion is very sensitive to the outside metal temperature. In the case of the Verdo outlet SH, similar lifetimes at a steam outlet temperature of 560°C will be expected if coated tubes are used for the hottest last 1/3 (8 m) of the tube length, as illustrated in figure 35.

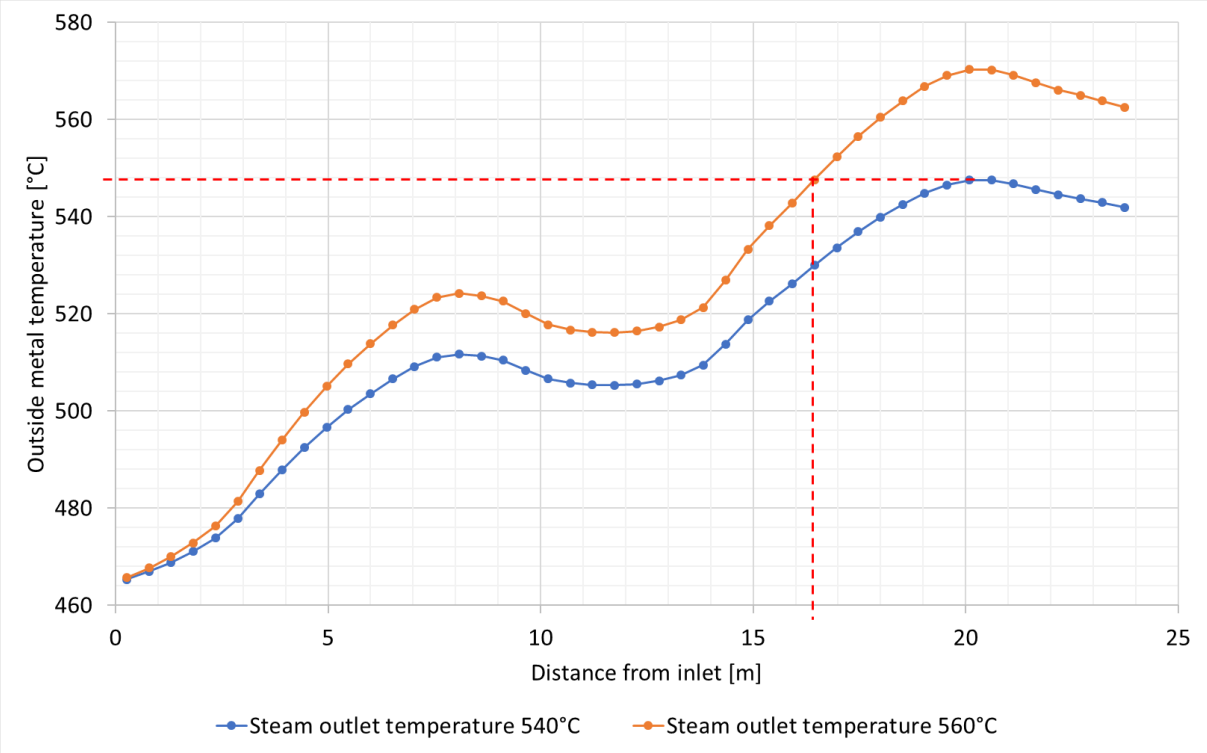

***Figure 33**: Outside metal temperature as a function of distance from SH inlet of the Verdo end SH, at an outlet steam temperature of 540° and 560°C.*

1.5.8.3 Repair concept

Tube leakage due to corrosion would not be expected with well performing coated tubes, but other factors e.g. foreign objects, sooth blower damage or flue gas erosion, might lead to the need for partial replacement of coated tubes. With un-coated tubes this is normally done by replacing the damaged tube length. This repair procedure means welding the replacement tube to the original tube. With coated tubes this could potentially lead to uncoated exposed welds in the high corrosive parts of the superheater, as in-situ coating techniques are generally much less reliable than work-shop techniques. Hence in these situations it would be best to replace the entire tube from inlet to outlet, which is much more expensive. With the sectioned design, it would only be necessary to replace the coated tube from outlet to the uncoated section of the tube, which would reduce the repair costs significantly, as e.g. the Verdo final SH where only 1/3 of the tube length would need coating.

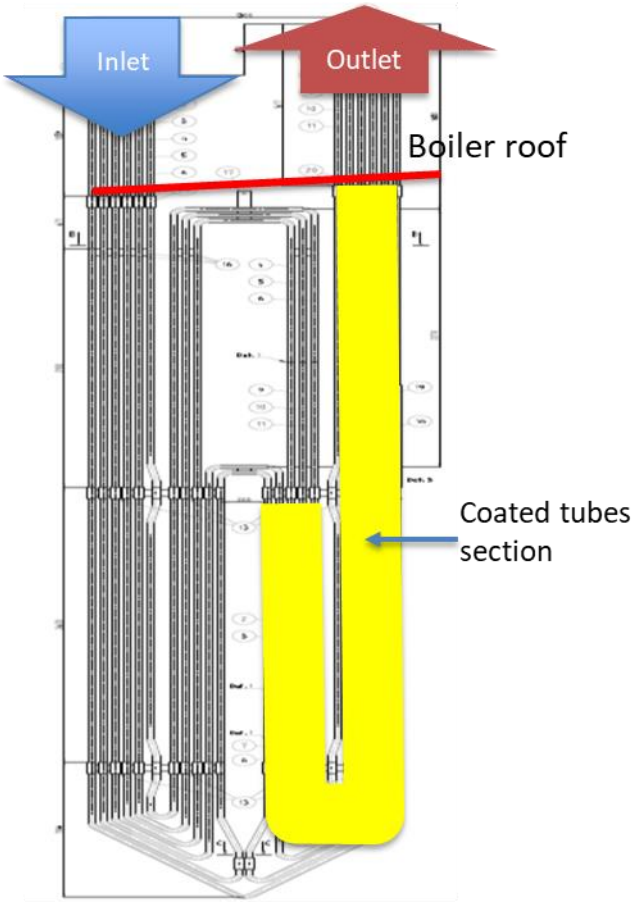

Figure 34: *Cross section of the Verdo final SH with indication of the section where metal temperatures would exceed the highest metal temperatures at steam outlet of 540° and where coatings must be used to obtain similar lifetimes at steam outlet temperatures of 560°C*

1.5.8.4 Fabrication costs

The fabrication of coated superheaters will be more expensive, both due to the extra fabrication step of the coating procedure, and materials cost for the coating material, which can be expensive especially if elements like e.g. Ni are used. As the coating techniques are not yet fully commercialised it is difficult to calculate the exact increase in fabrication costs. A conservative estimate would be a 30% increase compared to a similar austenitic non-coated SH. A SH for a medium sized biomass fired power plant as in case 2, similar to the Verdo boilers, adds up to a costs of approximately 3.5 MDKK[2], including fabrication and installation, with conventional non-coated austenitic SH materials. It is estimated that the total cost would be approximately 20 MDKK for a large-scale power plant like case 1. A 30% increase using coated tubes would mean a price increase of approximately 1 MDKK for the medium sized power plant and 6 MDKK for a large-scale power plant.

1.5.8.5 O&M costs

Based on the discussion above, the general O&M cost with coated tubes is not expected to increase. In case of unplanned outages due to tube leakages, lost revenue from heat and power sales, is many times the materials costs of the actual repair. Hence, the slightly increased materials cost for the coated tube and possibly longer tube sections to avoid welds in critical areas, are insignificant in such situations.

It is not expected that O&M (e.g. cleaning etc.) of coated tubes will be different from uncoated tubes. Before the tube tests it was suggested that the coated tubes might be less prone to slag build up, and therefore reduce the need for cleaning stops and increasing the

[2] According to BWSC

thermal efficiency of the boiler. However, the tube tests at Verdo and MSK did not confirm this. The buildup of slags and deposits were similar on the coated test tubes and on the original uncoated tubes.

1.5.8.6 Lifetime evaluation

The improved corrosion properties from protective coatings can be used to either extend the lifetime of superheaters operating in existing biomass CHP plants or to increase the steam parameters of new biomass units.

The CHP plant in Maribo Sakskøbing (MSK), which hosted one of the test tubes in the project, operates at an outlet steam temperature of 540°C. The plant was built in year 2000 and the outlet superheater was replaced in 2014 after approximately 80,000 operating hours. This means that the outlet superheater will be replaced two times during the plant lifetime.

1.5.8.7 Overall evaluation

- Increased steam parameters
The study has shown significant economic benefit from improved steam temperature on biomass fueled power plants. An increase in steam temperature from 540°C to 560°C on a new build medium sized biomass fueled power plant, could potentially save the utility owner 20 MDKK, in reduced fuel consumption over the design lifetime of the power plant (see table 8) under the assumption of constant heat and power output. If the increased steam temperature was used to increase the heat and power output from the same fuel consumption the potential economic benefit might be higher.

On large scale advanced USC power plants the potential lifetime savings from reduced fuel consumption is 355 MDKK if the steam temperature could be maintained at 580°C after conversion from coal to biomass. (see table 8)

Both for the medium sized and the large-scale power plant examples, the potential lifetime savings from increased steam temperatures, must be compared to the extra fabrication costs the coating procedure introduces.

It is assumed that coated SH at the increased steam temperatures have similar lifetime as un-coated superheaters at the current steam temperatures. This means that 3 final superheaters are still needed over the lifetime of the power plants at a 30% higher cost than the conventional un-coated superheaters. In table 8 the net lifetime savings are calculated for both power plant examples.

Table 8: *Potential lifetime savings (fuel savings-increased O&M costs)*

	Lifetime fuel savings	Increased O&M cost (SH exchange with coated tubes)	Net potential lifetime savings
Case 1	20 MDKK	3 x 1 MDKK= 3MDKK	17 MDKK
Case 2	355 MDKK	3 x 6 MDKK = 18 MDKK	337 MDKK

- *Increased lifetime*

In addition to significantly increased superheater corrosion, increased steam temperatures may also reduce lifetime of other critical boiler components (e.g. grate, membrane walls etc.). Even if the superheater corrosion issues are solved with coatings, boiler manufacturers might be reluctant to increase the steam temperature beyond the current 540°C maximum. Instead coatings could be used to increase the lifetime of superheaters operating at 540°C steam temperature. Increased lifetime of superheaters would decrease the operational risk for investors in new power plants.

If the operating life of superheaters at 540°C steam temperature could be increased so no superheater replacements would be necessary during the design life of the power plant, the operator would save the cost of two superheaters or approximately 7 MDKK for a medium sized power plant and 40 MDKK for a large scale power plant. The extra cost of the coated SH is estimated to approximately 1 MDKK and 6 MDKK for the medium sized and large-scale cases respectively, hence there is still an economical benefit.

The potential savings are obviously significantly lower than utilizing an increased corrosion resistance to increase the maximum allowable steam temperature. It would however still be worth chasing in this case, as increased operating life can give boiler manufactures a significant commercial advantage. Especially if the coatings are indifferent to the fuel specification, as there is a trend to utilize lower grade biomass (e.g. waste wood and virgin wood) due to shortages of wood chip and straw.

1.5.8.9 Conclusion from feasibility study

With the current best available materials, the maximum steam outlet temperature is limited to 540°C for biomass fired power plants. The study has shown the large economic benefits from increased steam outlet temperatures in biomass fired power plants. The test operation of the coated SH tubes in this project unfortunately showed that the test coatings were not inert to high temperature Cl corrosion occurring in biomass fired boilers. However, this study has shown that it is worth pursuing materials solutions to combat Cl induced corrosion in biomass fired boilers.

Increased corrosion resistance can also be utilized to increase the operational life of superheaters at the current maximum steam outlet temperature of 540°C. Even though the economic benefit is smaller in this case, it is still worth chasing, as increased operating life and reliability can give boiler owners and manufactures a significant commercial advantage. Especially if the coatings are indifferent to the fuel specification, as there is trend to utilize lower grade biomass (e.g. waste wood and virgin wood) due to shortages of wood chip and straw.

1.5.9 Dissemination of project results

Project results were disseminated between project partners at annual project meetings, where the planning of tube installations and removal were also discussed.

A website was set up for general information about the project:
http://www.biomasscoat.mek.dtu.dk/english

The scientific results from the project were disseminated through publication of three scientific papers produced as a part of the ph.d. project:

- *Duoli Wu, Sunday Chukwudi Okoro, Kristian Vinter Dahl, Melanie Montgomery, Karen Pantleon, John Hald "Laboratory investigations of Ni-Al coatings exposed to conditions simulating biomass combustion" Presented at 9th International Symposium on High-Temperature Corrosion and Protection of Materials, 2016.*
- *D. Wu, KV Dahl J.L Madsen, T.L Christiansen, M. Montgomery, J. Hald: "Effects of Different Fuel Specifications and Operation Conditions on the Performance of Coated and Uncoated Superheater Tubes in Two Different Biomass-Fired Boilers" Applied Energy Materials 1, Vol 4, (2018) pp. 1463-1475.*
- *D.L. Wu, K.V Dahl, T.L. Christiansen, M. Montgomery, J. Hald "Microstructural investigations of Ni and Ni2Al3 coatings exposed in biomass power plants" Materials at High Temperatures, Vol 35: 1-3, (2018) pp. 255-266.*

These papers can be accessed at the journal homepages against a fee. The papers are openly available in post print versions free of charge at www.orbit.dtu.dk

A ph.d. thesis was written and successfully defended:

- *Duoli Wu"Corrosion Resistant Coatings for Biomass Firing" Ph.d. Thesis, DTU Mechanical Engineering, February 2018, 222 pages*

The thesis is available in a printed version and will become available online at www.orbit.dtu.dk

The thesis contains manuscripts for three further papers, which are planned to be published in near future:

- *D.L. Wu, K.V Dahl, F. B. Grumsen, T.L. Christiansen, M. Montgomery, J. Hald "Characterization of Ni_2Al_3 coatings exposed in a biomass fired power plant using SEM, FIB and TEM"*
- *D.L. Wu, K.V Dahl, T.L. Christiansen, M. Montgomery, J. Hald "Corrosion behaviors of Ni and Ni_2Al_3 coatings exposed in a biomass fired power plant for two years"*
- *D.L. Wu, K.V Dahl, T.L. Christiansen, M. Montgomery, J. Hald "Corrosion performance of preoxidised Ni_2Al_3, CeO_2 dispersed Ni_2Al_3 and nitride coatings exposed in a biomass fired power plant*

Once published, the papers will become available for download in post print versions free of charge at www.orbit.dtu.dk

1.6 Utilization of project results

The overall goal of the project to demonstrate improved coating solutions for reduced biomass corrosion was not fulfilled, and thus the foreseen direct commercial exploitation will not be realised.

The project has, however, resulted in significantly improved understanding of huge gaps between corrosion and degradation mechanisms observed in real plant operation and in the necessarily simplified conditions in laboratory.

This understanding is not only highly useful to the scientific community, but also to plant owners and manufacturers, who are frequently approached by companies offering "solve it all" coating solutions based on laboratory testing. Their claims can be critically reviewed based on experiences from the present project.

As a consequence of the results, future materials R&D on materials for biomass corrosion must be based on tests with both harsher corrosion conditions and thermal cyclic loading of coatings in order to give realistic estimates of real plant performance.

The feasibility study has quantified the significant potential economic benefits to plant owners over plant lifetime (200,000 hours) from increased operating temperatures (10-300MDKK) and prolonged life (5-30MDKK) in biomass fired CHP plants. Potentially huge savings from avoided unplanned plant outages were not quantified. This demonstrates that it is certainly worthwhile to continue R&D on biomass corrosion, not only to realise lower cost of energy from biomass CHP, but also to give plant manufacturers a better competitive edge.

A ph.d. candidate Duoli Wu was educated in the project, and he is now employed as assistant professor at Yangzhou University in China, where he continues research on coating systems for corrosion protection and other applications. Research collaboration between DTU Mechanical Engineering and Yangzhou Unversity is foreseen.

Results from the project are used in teaching at DTU Mechanical Engineering both in scheduled courses and in student projects (B.Sc. and M.Sc).

1.7 Project conclusion and perspective

State of the art materials solutions for superheaters in biomass fired boilers are 18%Cr austenitic steels. Based on new understanding of corrosion mechanisms in biomass firing the present project aimed to develop and demonstrate new innovative coatings containing aluminium and/or nickel. Systematic small-scale laboratory tests had indicated that such coatings could significantly reduce corrosion rates in biomass fired power plants.

Coating processes were developed at DTU Mechanical Engineering and tube sections (200 mm length) were coated with Ni by electroplating and subsequently Al was diffused into the surface of the Ni plating by pack aluminizing.

Tubes sections coated with Ni and with NiAl were installed in the superheaters of two different biomass fired CHP plants at Refa Energi in Maribo Sakskøbing (MSK) and at Verdo in Randers. The plants were selected since they had very different operating conditions: Whereas MSK had daily start-stop cycles and operated at steam temperature up to 540ºC, Randers operated continuously at steam temperatures up to 520ºC with only few stops in the heating season. Also the plants fired different biomasses (Straw/grass seed chaff at MSK and Wood chips or pellets at Randers).

Added Values selected the specific installation sites in the plants based on superheater model calculations, which identified positions, where the most severe corrosion could be expected. BWE welded the tubes into the superheaters after approval of the experiment with the pressure vessel authorities (Arbejdstilsynet). Tubes were tested up to two years with partial replacement after one year.

Investigations of the extracted tubes showed that both the Ni and the NiAl coatings spalled at MSK during the first year of operation, most probably due to the highly intermittent operation, which leads to cyclic thermal stresses in the coatings and a predominantly mechanical failure.

At Randers, the NiAl coatings survived the first year of operation, due to lower temperature and less intermittent operation. However, during the second year of operation the NiAl coatings at Randers failed completely due to corrosion attack, which shows that the protective corrosion behavior seen in the laboratory could not be confirmed in plant.

The Ni coatings performed better in Randers, but they were found to offer only rather marginally reduced corrosion rates as compared to uncoated tubes.

As such the in-plant testing proved to be much harsher than the simplified laboratory testing. Thus, future materials development for improved corrosion resistance in biomass firing must consider tests in corrosive environments much closer to the conditions in real plant.

The improved understanding of loading conditions in real plant will provide input to design laboratory tests, which can give more realistic estimates of materials behavior in biomass firing.

A feasibility study by Added Values has quantified the considerable potential economic gains over plant lifetime, which can be foreseen with either improved efficiency (10-300 MDKK) or reduced O&M costs (5-30 MDKK) of biomass fired CHP plants based on improved materials. This demonstrates that it is certainly worthwhile to continue R&D on biomass corrosion, not only to realise lower cost of energy from biomass CHP, but also to give plant manufacturers a better competitive edge.

1.8 References

1. Montgomery, M., Jensen, S. A., Borg, U., Biede, O., Vilhelmsen, T., *Experiences with high temperature corrosion at straw-firing power plants in Denmark*. Materials and Corrosion 2011, 62(7): p. 593-605.
2. Montgomery. M., Karlsson, A., In-situ corrosion investigation at Masnedø CHP plant - a straw-fired power plant. Materials and Corrosion, 1999, 50: p. 579-584.
3. M. J. McNallan, W. W. Liang, S. H. Kim, and C. T. Kang, "Acceleration of the High Temperature Oxidation of Metals by Chlorine," in *High Temperature Corrosion, NACE*, 1983, pp. 316-321.
4. Li, Y.S., M. Spiegel, and S. Shimada, *Corrosion behaviour of various model alloys with NaCl-KCl coating.* Materials Chemistry and Physics, 2005. 93(1): p. 217–223.
5. Jonsson, T., et al., The influence of KCl on the corrosion of an austenitic stainless steel (304L) in oxidizing humid conditions at 600 ºC: A microstructural study. Oxidation of Metals, 2009. 72(3): p. 213–239.
6. Karlsson, S., et al., Alkali Induced High Temperature Corrosion of Stainless Steel: The Influence of NaCl, KCl and CaCl2. Oxidation of Metals, 2012. 78(1–2): p. 83–102.
7. Pettersson, C., J. Pettersson, H. Asteman, J.-E. Svensson and L.-G. Johansson *KCl-induced high temperature corrosion of the austenitic Fe-Cr-Ni alloys 304L and Sanicro 28 at 600°C.* Corrosion Science, 2005. 48(6): p. 1368–1378.
8. Lehmusto, J., Yrjas, P., Skrifvars, B.-J., Hupa, M., *High temperature corrosion of superheater steels by KCL and K2CO3 under dry and wet conditions*, Fuel Processing Technology, 2012. 101: p.253–261.
9. Kiamehr, S., Dahl, K.V., Lomholt, T. N., Christiansen, T. L., Somers, M.A.J., *High Temperature Corrosion due to Biomass Firing: A Study on the Reactivity between Potassium Chloride and Oxides*, Extended abstract submitted and approved for ISHOC 2014, International Symposium on High-Temperature Oxidation and Corrosion 2014, 23-27 June 2014. Hakodate, Hokkaido Japan.
10. https://www.energiforskning.dk/da/projects/detail?program=24&teknologi=11&field_bevillingsaar_value=&start=&slut=&field_status_value=done&keyword=GREEN&page=0 (Accessed 11/11/2018)
11. S. Kiamehr, *Materials Solutions to Mitigate the Alkali Chloride-Induced High Temperature Corrosion*, Ph.D Thesis DTU Mechanical Engineering, November 2014
12. S. Kiamehr, T.N. Lomholt, K.V. Dahl, T.L. Christiansen, M.A.J. Somers, Application of aluminum diffusion coatings to mitigate the KCl-induced high-temperature corrosion, Mater. Corros. (2016) 82–94.
13. K.V. Dahl, A. Slomian, T.N. Lomholt, S. Kiamehr, F.B. Grumsen, M. Montgomery, T. Jonsson, Characterization of pack cemented Ni2Al3 coating exposed to KCl(s) induced corrosion at 600 oC, Mater. High Temp. (2017).
14. Li, Y.S., Spiegel, M., Shimada, S., *Effect of Al/Si addition on KCl induced corrosion of 9% Cr steel*, Materials Letters, 2004, 58: p. 3787-3791.
15. Li, Y.S., Niu, Y., Spiegel, M. *High temperature interaction of Al/Si-modified Fe–Cr alloys with KCl*. Corrosion Science, 2007, 49(4): p. 1799-1815.
16. Shinata, Y., Takahashi, F., Hashiura, K., *NaCl-induced Hot Corrosion of Stainless Steels*. Materials Science and Engineering, 1987, 87: p. 399-405.
17. Hiramatsu, N., Uematsu, Y., Tanaka, T., Kinugasa, M., *Effects of Alloying Elements on Nacl-induced Hot Corrosion of Stainless Steels*. Materials Science and Engineering, 1989, A120: p. 319-328.
18. Sato, N., Kaneta, T, Fukumoto, M., Hara, Motoi, High Temperature Corrosion Resistance of Siliconized Stainless Steel under Continuous Deposition of Salt, Materials Science Forum, 2011, 696: p. 266-271.
19. Jonsson, T. Slomian, A., Lomholt, T. N., Kiamehr, S. Dahl, K. V., *Microstructural investigations of Ni/Ni2Al3 exposed to KCl(s) induced corrosion at 600°C*, submitted to and accepted for oral presentation at Microscopy of Oxidation 9, 9th International Conference - 14-16 April 2014 - University of Nottingham, UK.
20. O.H. Larsen, M. Montgomery, Materials problems and solutions in biomass fired plants, Energy Mater. 1 (2006) 227–237.
21. Xiang, Z.D., Datta, P.K., Effects of pack composition on the formation of aluminide coatings on alloy steels at 650°C, Journal of Materials Science, 2005. 40: p. 1959-1966.
22. Xiang, Z.D., Rose, S.R., Datta, P.K., Long-term oxidation kinetics of aluminide coatings on alloy steels by low temperature pack cementation process. Journal of Materials Science, 2006. 41: p. 7353-7360.
23. Wang, J., Wu, D.J., Zhu, C.Y., Xiang, Z.D., Low temperature pack aluminizing kinetics of nickel electroplated on creep resistant ferritic steel. Surf. Coat. Technol, 2013. 236: p. 135-141.
24. Rohr, V., Schütze, M., Fortuna, E., Tsipas, D.N., Milewska, A., Pérez, F.J., Development of novel diffusion coatings for 9 – 12 % Cr ferritic-martensitic steels, Materials and Corrosion 2005. 56(12): p. 874-881.

25. Aguero, A., Muelas, R., Pastor, A., Osgerby, S., Long exposure steam oxidation testing and mechanical properties of slurry aluminide coatings for steam turbine components, Surf. Coat. Technol. 2005. 200: p. 1219–1224.
26. https://www.materials.sandvik/en/materials-center/material-datasheets/
27. Wu, D. J. *Corrosion Resistant Coatings for Biomass Firing*, Ph.d. Thesis, DTU Mechanical Engineering, February 2018, 222 pages
28. Duoli Wu, Sunday Chukwudi Okoro, Kristian Vinter Dahl, Melanie Montgomery, Karen Pantleon, John Hald "Laboratory investigations of Ni-Al coatings exposed to conditions simulating biomass combustion" Presented at 9th International Symposium on High-Temperature Corrosion and Protection of Materials, 2016.
29. S.S. Petersen, CFD Modelling of a Biomass Incinerator for Prediction of Risk Areas for Corrosion Damages, master thesis, Technical University of Denmark, 2012.
30. Phyllis2 database for biomass and waste, https://www.ecn.nl/phyllis2, Energy research Centre of the Netherlands.
31. N. Henriksen, T. Vilhelmsen, O.H. Larsen, R. Blum, Oxide growth and temperature increase in evaporators of supercritical PF boilers, VGB Powertech. 79 (1999) 71–77.
32. L. Delaey, H.Tas, Hot Isostatic Pressing 93, in: Elsevier Science B.V, Amsterdam, 1994: pp. 301–308.
33. S.C. Okoro, M. Montgomery, K. Pantleon, High temperature corrosion under laboratory conditions simulating biomass-firing: a comprehensive characterization of corrosion products, Energy Fuels. 28 (2014) 6447–6458
34. M. Broström, S. Enestam, R. Backman, K. Mäkelä, Condensation in the KCl-NaCl system, Fuel Process. Technol. 105 (2013) 142–148.
35. D. Lindberg, J. Niemi, M. Engblom, P. Yrjas, T. Laurén, M. Hupa, Effect of temperature gradient on composition and morphology of synthetic chlorine-containing biomass boiler deposits, Fuel Process. Technol. 141 (2016) 285–298.
36. P.A. Jensen, F.J. Frandsen, K. Dam-Johansen, B. Sander, Experimental investigation of the transformation and release to gas phase of potassium and chlorine during straw pyrolysis, Energy Fuels. 14 (2000) 1280–1285.
37. O.H. Larsen, J.P. Jensen, O. Biede, M. Montgomery, C. Andersson, Relations between combustion, deposition, flue gas temperatures and corrosion in straw-fired boilers., in: 2nd World Conf. Technol. Exhib. Biomass Energy Ind., Rome, 2004: p. OD7.2.
38. H. Zhou, P.A. Jensen, F.J. Frandsen, Dynamic mechanistic model of superheater deposit growth and shedding in a biomass fired grate boiler, Fuel. 86 (2007) 1519–1533.
39. J. Pettersson, N. Folkeson, L.G. Johansson, J.E. Svensson, The effects of KCl, K2SO4 and K2CO3 on the high temperature corrosion of a 304-type austenitic stainless steel, Oxid. Met. 76 (2011) 93–109.
40. Z. Wen, Y. Zhao, H. Hou, J. Tian, P. Han, First-principles study of Ni-Al intermetallic compounds under various temperature and pressure, Superlattices Microstruct. 103 (2017) 9–18.
41. M.S.A. Karunaratne, S. Kyaw, A. Jones, R. Morrell, R.C. Thomson, Modelling the coefficient of thermal expansion in Ni-based superalloys and bond coatings, J. Mater. Sci. 51 (2016) 1–14.
42. H.P. Nielsen, F.J. Frandsen, K. Dam-Johansen, L.L. Baxter, Implications of chlorine-associated corrosion on the operation of biomass-fired boilers, Prog. Energy Combust. Sci. 26 (2000) 283–298.
43. H.J. Grabke, E. Reese, M. Spiegel, The effects of chlorides, hydrogen chloride, and sulfur dioxide in the oxidation of steels below deposits, Corros. Sci. 37 (1995) 1023–1043.
44. H.H. Krause, High temperature corrosion in waste incineration systems, J. Mater. Energy Syst. 7 (1985) 322–332.
45. K. Salmenoja, K. Makela, Prevention of superheater corrosion in the combustion of biofuels, Proceedings of NACE Corrosion. (2000).
46. S.C. Okoro, M. Montgomery, F.J. Frandsen, K. Pantleon, Effect of Water Vapor on High-Temperature Corrosion under Conditions Mimicking Biomass Firing, Energy Fuels. 29 (2015) 5802–5815.
47. J. Pettersson, J.E. Svensson, L.G. Johansson, KCl-Induced Corrosion of a 304-type Austenitic Stainless Steel in O2 and in O2 + H2O Environment: The Influence of Temperature, Oxid. Met. 72 (2009) 159–177.

48. S.C. Okoro, S. Kiamehr, M. Montgomery, F.J. Frandsen, K. Pantleon, Effect of flue gas composition on deposit induced high temperature corrosion under laboratory conditions mimicking biomass firing. Part I: Exposures in oxidizing and chlorinating atmospheres, Mater. Corros. 68 (2017) 499–514.
49. M. Montgomery, A. Karlsson, O.H. Larsen, Field test corrosion experiments in Denmark with biomass fuels Part I: Straw-firing, Mater. Corros. 53 (2002) 121–131.

Annex

Relevant links:

Homepage with general information about the project:

http://www.biomasscoat.mek.dtu.dk/english

Direct link to published papers with open access:

http://orbit.dtu.dk/en/publications/search.html?search=Duoli+Wu&uri=&advanced=true&institution=dtu&organisationName=&organisations=&type=&publicationstatus=&publicationcategory=&peerreview=&publicationYearsFrom=&publicationYearsTo=&submissionYearsFrom=&submissionYearsTo

The ph.d. Thesis and further published papers will become available here in near future.